TEMPERATURE DISTRIBUTION IN A FLUID FLOWING THROUGH AN ANNULUS WITH AXIAL VARIATION IN HEAT FLUX

by

Peter Paul Zemanick

A Thesis Submitted to the
Graduate Faculty in Partial Fulfillment of
The Requirements for the Degree of
MASTER OF SCIENCE

Major Subject: Nuclear Engineering

Approved:

Iowa State University
Of Science and Technology
Ames, Iowa

1961

TABLE OF CONTENTS

I. INTRODUCTION

The primary objective of this investigation was to develop a suitable method for determining the temperature at any point in a fluid flowing turbulently through a heated annulus. The core of the annulus is considered to enclose the heat source, while the outer cylinder is assumed perfectly insulated.

The annulus represents no uncommon geometry in modern heat exchanging equipment, and, therefore, the engineering applications of the analysis presented are legion. The apparatus of particular interest to the author, and one which manifests the property of axial heat load variation according to a reasonably predictable distribution, is the nuclear reactor. The annulus is a frequently found configuration of reactor coolant channel, with the annulus core the fuel element and heat source. Ideally, the heat flux from this element follows a "chopped" cosine variation, symmetric about the longitudinal mid-point of the fuel rod. Approximate solutions to various degrees of accuracy are proposed for just this variation. As an example, see Hall (10). The presence of control and structural elements can distort this rather simple variation. Furthermore, this heat load distribution is sometimes intentionally changed. The purposes for such a change are to provide more nearly uniform heat transfer along the channel, and to avoid a radical difference among core temperatures at various

stations along the channel. The most direct means of adjusting the heat flux variation is to use nuclear fuel of varying enrichments as one proceeds along the fuel element. In any case, the nuclear reactor coolant channel is one example of an annular passage which can be heated according to a diversity of axial heat load distributions. Consequently, the reactor heat transfer analyst must be able to predict from design data the heat transfer characteristics of such annular coolant channels with potentially complex patterns of heat addition. This paper offers one means of solution to such a problem.

The most significant aspect of the analysis is that the heat load is allowed to vary axially according to any arbitrary flux distribution. The most important assumptions are that fluid properties are considered constant and that steady-state conditions prevail.

A detailed analysis and derivation is followed by a step-by-step presentation of the mechanics of applying the equations to a specific problem. The method is applied to a more or less typical heat transfer situation and the results are presented and discussed. Finally, modes of further refinement of the method of solution are discussed.

The bulk of the thesis is not intended to apply to liquid metals. These are fluids, but fluids uniquely different from gases and the common liquids. The principal peculiarity is that of the large value of thermal conductivity compared with that of other common fluids. For a specific discussion of heat transfer to liquid metals, see Martinelli (14).

II. LIST OF SYMBOLS

c_p	Specific heat of fluid at constant pressure, BTU/(lb)(°F)
d	Diameter of circular channel, ft
g	Gravitational constant, 32.2 ft/sec^2
h	Film heat transfer coefficient, BTU/(sec)(sq ft)(°F)
k	Thermal conductivity of fluid, BTU/(sec)(sq ft)(°F/ft)
p	Static pressure, lb/sq ft
q	Rate of heat transfer per unit area, BTU/(sec)(sq ft)
q_1	Rate of heat transfer from wall of inner cylinder per unit area, BTU/(sec)(sq ft)
r	Radius, ft
r_{max}	Radius of maximum velocity, ft
T	Temperature at a point, °F
u	Time-averaged velocity parallel to wall at a point, ft/sec
u_m	Mean time-averaged velocity parallel to wall of fluid in entire channel, ft/sec
$\dot{w}$	Weight rate of flow, lb/sec
x	Axial distance along annulus, ft
y	Normal distance from wall, ft
ϵ_M	Coefficient of eddy diffusivity for momentum, sq ft/sec
ϵ_H	Coefficient of eddy diffusivity for heat, sq ft/sec
μ	Absolute viscosity of fluid, (lb)(sec)/sq ft
ρ	Mass density, (lb)(sec^2)/ft^4

τ Shear stress in fluid, lb/sq ft

Dimensionless quantities:

n Constant, 0.109

Pr Prandtl number, $c_p \mu g/k$

Re Reynolds number, $\frac{\rho u_m d}{\mu}$

$(Re)_2$ Modified Reynolds number, defined by Eq. 11

R_1^+ Inner-tube radius parameter, defined by Eq. 25

u^+ Velocity parameter, $\frac{u}{\sqrt{\frac{\tau_w}{\rho}}}$

y^+ Wall-distance parameter, $\frac{\sqrt{\frac{\tau_w}{\rho}}}{\frac{\mu}{\rho}} y$

κ Kármán constant, 0.36

Subscripts:

w Pertaining to a wall

1 Pertaining to inner cylinder or to region between inner cylinder and radius of maximum velocity

2 Pertaining to outer cylinder or to region between radius of maximum velocity and outer cylinder

III. BACKGROUND MATERIAL

Investigators have been unsuccessful thus far in their efforts to formulate a complete analytic description of the turbulent flow field. The principal difficulty lies in the random mixing which is characteristic of turbulence. From point of view of pure description of the fluctuating motions of turbulent flow, statistical methods seem to offer the most promise. However, the analyses that have been most valuable in terms of relationships which lead most readily to the solution of engineering problems involving fluid flow and heat transfer under turbulent conditions, have been analyses based on more nearly conventional fluid dynamics methods. These analyses have not been successful enough to yield complete solutions, but, in combination with carefully evaluated experimental data, have in many instances provided the engineer with tools for acceptably accurate results. The principal point to be made is that turbulent flow is so complex a physical occurrence that a complete mathematical description has not yet been formulated. Therefore, at least for the present, engineering problems involving turbulent conditions must be solved by what are, at best, semi-empirical relationships. For a review of the present level of knowledge related to turbulent phenomena, see Bird *et al.* (2), Ferrari (9), and Schlichting (20). Literature more directly applicable to the present investigation will be referred to in the body of this paper.

The characteristics of turbulent flow as it exists in channels have been extensively investigated. By obvious reasons of geometrical and experimental convenience, the bulk of this work has been done with channels of circular cross-section. Data on wall-to-wall velocity profiles, for instance, have been gathered over a broad range of Reynolds numbers. Technical progress both in clearer definitions of flow conditions as well as in reliable, precise measuring apparatus has led to a reassuring agreement of results from various investigators of recent years. Moreover, temperature profile data are not lacking. On the basis of all these efforts, semi-empirical relationships now exist that give easily accessible results (well-correlated by experimental data) which dependably describe radial temperature and velocity distributions for fully developed turbulent flow in circular channels. Moreover, analysis has progressed to the point of solutions for temperature and velocity distributions in the longitudinal direction also, but only for the simplest sort of temperature or heat flux distributions along the channel walls. Certain of these methods are briefly described in Knudsen and Katz (13, pp. 426-436). However, solutions that allow for an arbitrary axial distribution of temperature at, or heat flux from, the channel wall are notably absent.

While a comprehensive effort has been devoted to the investigation of turbulent flow in cylindrical channels and of turbulence in general, no significant accumulation of data

exists for turbulent flow in annular channels. Barrow (1) gives some sound reasons for investigators' preference for the circular channel. In the first place, concerning a pure analysis, the very geometry of the concentric annulus markedly complicates the relationships. Secondly, there is some controversy over the definition of "characteristic length" in the annulus, with different interpretations being favored by the significance of the different commonly used dimensionless ratios, i. e. Reynolds, Nusselt and Peclet numbers. Thirdly, there is the difficulty presented by the mechanical supports which must keep the annulus walls exactly concentric without noticeably disturbing flow in the test section. Finally, measurements in the fluid near the core wall practically have to be taken by a probe that passes through the outer wall and extends across the entire flow channel. Accuracy of data taken near the core wall (i. e., in the so-called laminar sublayer) is compromised by the presence of the flow-obstructing probe. Of course, some data are available, in spite of these obstacles. A comparison of two sets of data, Rothfus for air and Knudsen for water, is made by Knudsen and Katz (13, pp. 190-191). The comparison itself, or, rather, the discrepancies in the comparison, points to the need for additional data. Davis (3) amassed most of the then (1943) published data and attempted to correlate the data. However, his results remain little used.

To go on from a discussion of experimental data on radial

temperature and velocity distributions in annuli, to the matter of a solution to the complete channel problem, where heat can be supplied to the fluid according to any axial variation of heat flux, is to enter an area hardly touched by attempted analyses or experimental investigation. Tribus et al. (21) offer the only known published solution to this problem. The scheme of the solution presented in the present paper differs markedly from that of Tribus, and the semi-empirical equations that are called upon at various points in the analysis are, in the author's opinion, better substantiated by experimental data than are those used in the reference cited above. Naturally, the ultimate test of the methods would have to be made in carefully planned laboratory experiments. Such experiments would have to cope with the difficulties mentioned earlier in addition to the formidable requirement of supplying heat to the fluid through the annulus core and/or outer wall according to a precisely known axial heat flux distribution.

IV. BASIC RELATIONSHIPS

A. Introductory Concepts

The problem and its principal assumptions will be stated in detail. The geometry is that of a concentric, smooth annulus. Fluid flow is considered fully turbulent; this excludes the influence of so-called "end effects", which account for the laminar and transition regions through which the boundary layer develops until the layers from each wall meet at the radial point of maximum velocity. The outer wall is assumed to be perfectly insulated. Heat is supplied from the inner wall or core according to a known axial distribution.

The coolant properties are evaluated at the inlet temperature and assumed constant throughout the channel. This assumption, of course, discounts the effects of temperature and compressibility. In most cases, temperature effects are the more significant of the two. Pressure effects on fluid viscosity, thermal conductivity, and specific heat are negligible below critical pressure (over thirty atmospheres for air, for instance). High velocity effects are ignored, since the closed system being considered is not ordinarily designed for near sonic, much less supersonic velocities.

It will be helpful to an understanding of the development to have in mind a general conspectus of the line of attack.

In light of the paucity of data on fluid flow in annuli, one is forced to revert, as an expedient, to circular channel

data, supported as it is by extensive and painstaking experimentation, and to exploit such data generously in annulus problem solutions. The velocity profile of channeled turbulent flow is in the general shape of a flattened parabola. Velocity at the walls is zero. Maximum velocity in a circular channel is at the channel axis. Maximum velocity in the annular passage exists at a radial distance not midway between the walls but somewhat nearer the core wall. See Figure 1. The location of this distance is a function of the ratio of the shear stresses at the inner and outer walls of the annulus; the relation between these values will be derived later in the paper. The following explains the customary manner of applying cylindrical data to annular geometry. Figure 1 depicts the idea discussed. Let r_1 be the inner radius of the annulus and r_2, the outer radius; let r_{max} denote the radius of maximum velocity. The velocity profile between r_2 and r_{max} is assumed identical with the "top half" of the profile (under the same conditions of wall stress, fluid properties, and flow rate) in a circular tube of radius, $r_2 - r_{max}$. The velocity profile from the core to r_{max} is assumed identical with the "lower half" of the profile in a circular tube with radius, $r_{max} - r_1$. The assumption is most valid from r_2 inward, for this region might well be imagined as the outer portion of circular pipe flow. However, by the same comparison with the circular pipe condition, less validity can be expected of this assumption as it refers to the region between r_1 and r_{max}, for

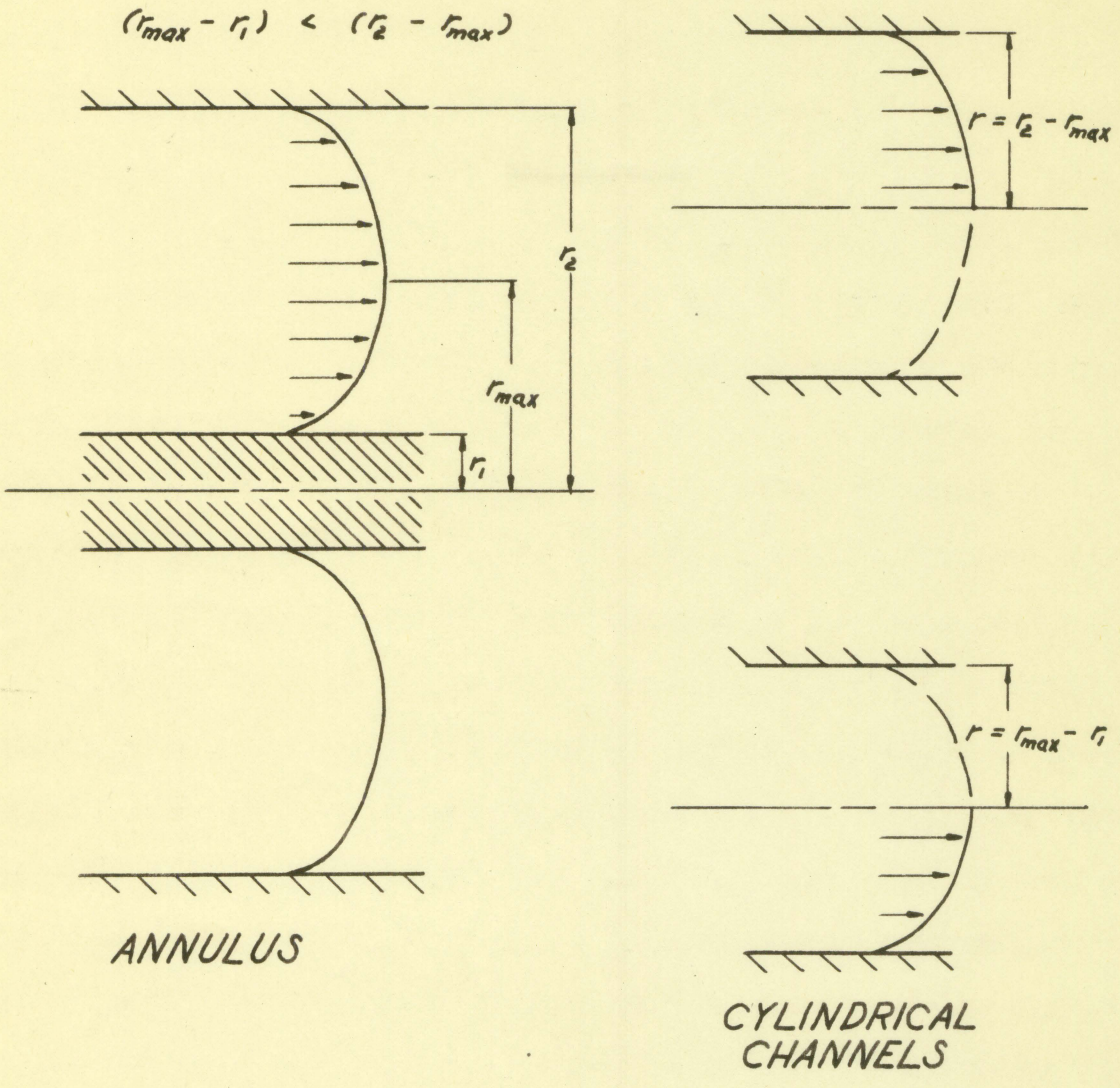

Figure 1. Annulus velocity profile

the core wall is, in a manner of speaking, in reverse curvature to that of its cylindrical counterpart. In tacit acknowledgement of this fact, there is a preponderant influence of r_2 to r_{max} flow conditions in the calculation of shear stress for both walls. (See Eq. 10.)

A distinctive characteristic of turbulence is the "eddy diffusivity". This concept purports to account for the transfer of heat and momentum due to turbulent mixing. This mixing is viewed as the random motion of parcels of fluid, each parcel carrying with it the temperature and momentum it possessed in its previous location. The laminar velocity profile is found to be parabolic in shape, that of turbulent flow, a flattened parabolic shape. The reason for the difference is that the constant interchange of fluid parcels, parcels of high velocity into lower velocity regions, and comparatively low velocity parcels in the opposite direction, tends to produce the zero slope velocity profile of "slug" flow. The uniform velocity condition is never achieved, but a profile of less curvature than that of a parabola is found. Turbulent heat transfer is similarly accomplished, in such a way that, in most of the channel, heat transport away from the walls and into the coolant by turbulent mixing is much more significant than transport by intermolecular conduction. This explains, in simple terms, the distinct advantage, from heat transfer considerations, of turbulent coolant flow. The improvement is sufficient to warrant (within limits) deliberate means of

inducing turbulence, even though the price of increased pumping power is inevitably exacted in such cases.

Mathematically, the effects of eddy diffusivity are expressed as shown below. Eddy diffusivity, as it affects momentum transfer, is regarded as analogous to viscosity, and, consequently, is often called "eddy viscosity". For heat transfer, the diffusivity is treated analogously to thermal conductivity; hence the terminology, "eddy conductivity".

Let τ = shear stress

μ = viscosity

u = velocity in the axial direction

y = radial distance from the wall

ϵ_M = eddy viscosity

The expression for total shear stress, due both to viscous shear and turbulence is

$$\tau = \mu \frac{du}{dy} + \rho \epsilon_M \frac{du}{dy} \qquad (1)$$

In like manner, let

q = radial rate of heat transfer

k = thermal conductivity

T = temperature

ρ = fluid density

g = gravitational constant

c_p = specific heat at constant pressure

ϵ_H = eddy conductivity

The total rate of heat transfer is

$$q = -k \frac{dT}{dy} - \rho g c_p \epsilon_H \frac{dT}{dy} \qquad (2)$$

The similarity between Eqs. 1 and 2 is plainly seen. Based on this similarity and some further manipulation of the equations, the Prandtl analogy was formulated. The Prandtl analogy states that the eddy conductivity and eddy viscosity are equal for fluids with a Prandtl number of one. The analogy is extended to include fluids of Prandtl number nearly one (e. g., $Pr_{air} \simeq .73$). This assumption, if accepted, significantly simplifies turbulent heat transfer analysis. Although the conclusion seems almost arbitrary, reasonably accurate results have been consistently obtained and analytic efforts considerably expedited. For discussions of the validity of the Prandtl analogy, see Reichardt (17, pp. 14-17) and Schlichting (20, pp. 498-499).

Therefore, if eddy viscosity can be determined, eddy conductivity is known (by the Prandtl analogy). Thus, one has at hand most of the tools necessary for solving the turbulent convective heat transfer problem.

The "similarity rule" of von Kármán assumes that turbulent fluctuations at all points of the field of flow are similar, i. e. they differ from point to point only as far as length and time scale factors are concerned. Based on mathematical conclusions drawn from this hypothesis, von Kármán (12) expresses shear stress in the turbulent stream as

$$\tau = \rho \kappa^2 \frac{\left(\frac{du}{dy}\right)^4}{\left(\frac{d^2u}{dy^2}\right)^2} \qquad (3)$$

In arriving at Eq. 3, it was assumed that viscous shear is negligible in the principal flow region. Therefore,

$$\rho \kappa^2 \frac{\left(\frac{du}{dy}\right)^4}{\left(\frac{d^2u}{dy^2}\right)^2} = \rho \epsilon_M \frac{du}{dy}$$

Or

$$\epsilon_M = \kappa^2 \frac{\left(\frac{du}{dy}\right)^3}{\left(\frac{d^2u}{dy^2}\right)^2} \qquad (4)$$

where κ is a constant to be evaluated experimentally.

To solve for velocity as a function of y, radial position away from the wall, von Kármán integrated Eq. 3. However, prior to the integration, the expression for shear stress was modified so as to be expressed in universally applicable dimensionless parameters. These parameters are, by definition,

$$u^+ = \frac{u}{\sqrt{\frac{\tau_w}{\rho}}}$$

$$y^+ = \frac{\sqrt{\frac{\tau_w}{\rho}}}{\frac{\mu}{\rho}} y$$

The important integrated expression is

$$u^+ = C + \frac{1}{K} \ln y^+ \qquad (5)$$

where τ_w = shear stress at the wall

C = constant of integration

Various values for the constants, C and K, have been prescribed by different workers. The most widely accepted values are due to Deissler (4), and these values are

$$C = 3.8$$

$$K = 0.36$$

Equation 5 has been proven valid everywhere in the channel except near the channel wall.

Deissler (4) has deduced that, while shear stress away from the wall may be a function, not of u and y, but only of the changes in velocity in the vicinity of a point (cf. Eq. 3), shear stress near the wall is influenced by u and y proper. By a dimensional analysis, Deissler arrived at the following relationship for eddy viscosity

$$\epsilon_M = n^2 u y \qquad (6)$$

where n has been evaluated experimentally as 0.109.

Equation 1 can be rewritten as

$$\tau = \mu \frac{du}{dy} + \rho n^2 u y \frac{du}{dy} \qquad (7)$$

Equation 7 can be written as a function of u^+ and y^+, rather than of u and y, and integrated. The resultant expression describes the velocity-distance relationship in the region near the channel walls

$$y^+ = \frac{1}{n} \frac{\frac{1}{\sqrt{2\pi}} \int_0^{nu^+} e^{\frac{-(nu^+)^2}{2}} d(nu^+)}{\frac{1}{\sqrt{2\pi}} e^{\frac{-(nu^+)^2}{2}}} \qquad (8)$$

where $\frac{1}{\sqrt{2\pi}} e^{\frac{-(nu^+)^2}{2}}$ is the normal error function of $n\,u^+$. Tabulated numerical values of the integral for any $n\,u^+$ appear in most compilations of statistical tables.

Equation 5 is assumed to apply in the region away from the wall or in the main flow area, while Eq. 8 is assumed to describe the velocity distribution in the vicinity of the wall. The reason for treating the fluid in the channel as though two separate flow regimes exist is that both laminar and turbulent flow conditions are present, each with its characteristic mechanisms of momentum and heat transport. Not that distinct laminar and turbulent regions can be delineated, for only the flow immediately adjacent to the wall is completely laminar, and only that in the central portion of the flow area, completely turbulent. Between is a buffer layer which is neither entirely laminar nor entirely turbulent. Deissler's experiments have indicated that the point of transition from Eq. 8 to Eq. 5 (and from Eq. 6 to Eq. 4) is at y^+ of 26. Figure 2 illustrates the division of an annular flow channel into the regions just described. The figure cannot adequately represent the relative sizes of the zones. Under

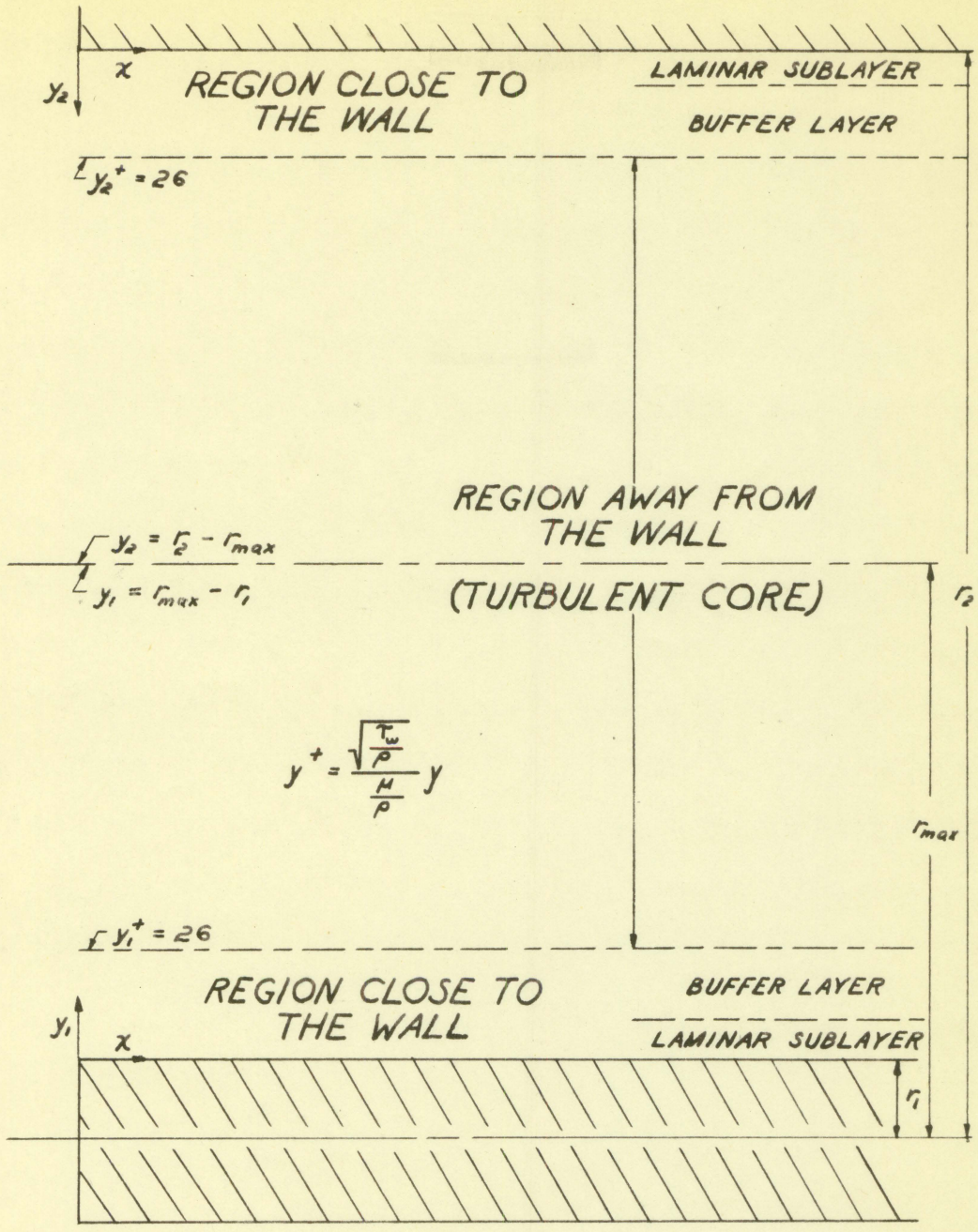

Figure 2. Division of the channel into flow regions

normal flow conditions, the transition region occupies an extremely narrow portion of the entire channel, with the laminar sublayer even more narrow (to y^+ of approximately 3).

Equations 5 and 8 are the governing equations for a plot of u^+ versus y^+, and this plot is commonly referred to as the universal velocity profile. This combination of Eqs. 5 and 8 gives a curve with a slope discontinuity at the transition point, but a curve, nonetheless, which has been impressively validated by experimental data over a Reynolds number range of 8,000 to 220,000. See Deissler and Taylor (6, p. 26). The analysis will utilize these experimentally established relationships.

Turning from fluid shear and the velocity distribution to the skin friction at the channel walls, there is yet another useful relationship stemming from the von Kármán similarity rule. The form of the equation is von Kármán's; the constants have evolved to their present values.

$$\frac{u_m}{\sqrt{\frac{2\tau_w}{\rho}}} = 4.0 \log \frac{Re}{u_m}\sqrt{\frac{2\tau_w}{\rho}} - 0.40 \qquad (9)$$

where u_m = average velocity

Re = Reynolds number = $\frac{u_m \rho d}{\mu}$, where d is the tube diameter. See Knudsen and Katz (13, p. 176).

As with the earlier formulae, Eq. 9 was originally derived for turbulent flow through a cylindrical cross section.

While circular channel velocity distributions can be applied directly to annular cases (even though in piecemeal fashion, as depicted in Figure 1), the equation for shear stress (Eq. 9) must be modified. As will be seen when the force equations are derived, shear stress at the outer wall (henceforth designated τ_2) and that at the core (τ_1) differ considerably. Monrad and Pelton (16) point out the necessity of accounting for this difference in calculating skin friction. Once the radius of maximum velocity is known, the ratio of τ_1 and τ_2 is known. Therefore, the solution for skin friction at one boundary readily leads to a value for the other. Equation 9 was modified by Rothfus et al. (18 and 19) to solve for shear stress at the outer wall. Recall that fluid in the annular channel is imagined to move in two separate flow regions, namely, between r_1 and r_{max}, and between r_{max} and r_2. For the reason advanced earlier, it is likely that our description of dynamic conditions in the outer region of flow (i. e., r_{max} to r_2) is a more accurate description than that deduced for the inner region. It is logical, therefore, that Rothfus and his coworkers preferentially deal with the former region. Their relationship is

$$\frac{u_m}{\sqrt{\frac{2\,\tau_2}{\rho}}} = 4.0 \log \frac{(Re)_2}{u_m} \sqrt{\frac{2\,\tau_2}{\rho}} - 0.40 \quad (10)$$

where

$$(Re)_2 = \frac{2\,(r_2^2 - r_{max}^2)\,u_m \rho}{r_2\,\mu} \qquad (11)$$

It is obvious that Eq. 10 must be solved by iteration or by graphical means. The equation is confirmed reasonably well by experimental data presented by its originators.

To review, this section has dealt with the velocity profile, eddy viscosity, eddy conductivity, and wall shear stress as they apply to turbulent, channeled flow.

These basic notions lay sufficient groundwork for derivation of the heat and force equations used to solve the particular problem of interest in this investigation.

B. Heat Transfer Equation

1. The basic equation

The annular fluid element of Figure 3 is to be analyzed in terms of the heat accumulated in it. An annular shaped element can be conveniently used since there is no angular variation of conditions, i. e., all fluid and thermal properties are assumed symmetric about the longitudinal axis of the channel.

Let dA be the frontal area of the fluid element, i. e., $2\pi r\,dr$. Let dS be the inner surface which is normal to radial lines from the channel axis, i. e., $2\pi r\,dx$.

The heat entering the fluid element may be expressed as the sum of three terms:

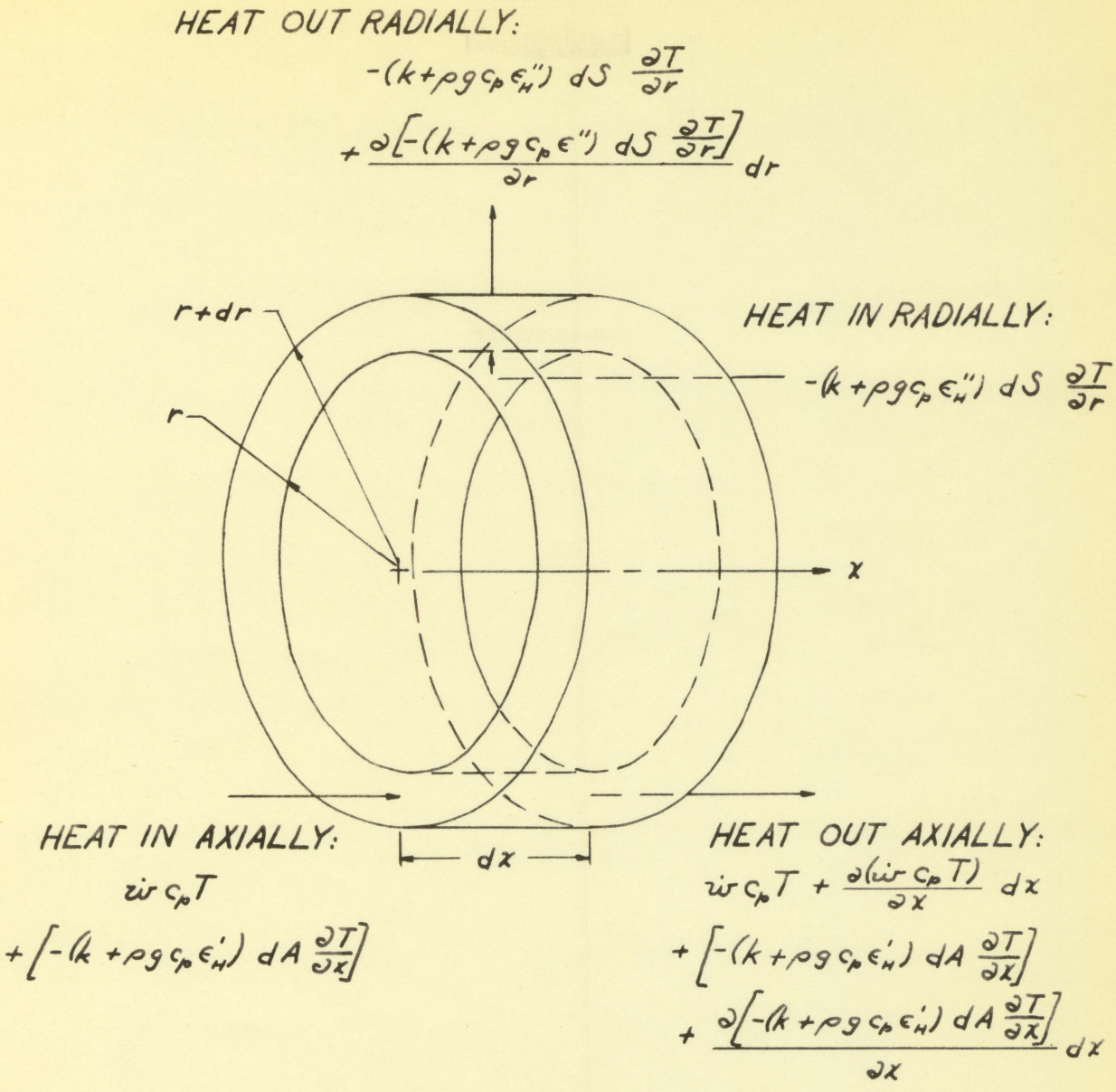

Figure 3. Heat balance in an annular fluid element

$\dot{w}\, c_p\, T$ (convective heat transfer in the axial direction, $\dot{w}$ being the weight rate of flow)

$$+ \left[-(k + \rho g c_p \epsilon'_H)\, dA \frac{\partial T}{\partial x}\right]$$ (conductive and turbulent heat transfer in the axial direction)

$$+ \left[-(k + \rho g c_p \epsilon''_H)\, dS \frac{\partial T}{\partial r}\right]$$ (conductive and turbulent heat transfer in the radial direction)

Note that the eddy conductivity is denoted by ϵ'_H as it refers to heat transport in the axial direction, and by ϵ''_H, in the radial direction. The distinction is made because no reason exists in this case to assume isotropic eddy diffusivity.

The heat leaving the element is

$$\dot{w} c_p T + \frac{\partial(\dot{w} c_p T)}{\partial x} dx + \left[-(k + \rho g c_p \epsilon'_H)\, dA \frac{\partial T}{\partial x}\right]$$

$$+ \frac{\partial\left[-(k + \rho g c_p \epsilon'_H)\, dA \frac{\partial T}{\partial x}\right]}{\partial x} dx$$

$$+ \left[-(k + \rho g c_p \epsilon''_H)\, dS \frac{\partial T}{\partial r}\right]$$

$$+ \frac{\partial\left[-(k + \rho g c_p \epsilon''_H)\, dS \frac{\partial T}{\partial r}\right]}{\partial r} dr$$

The rate at which heat is accumulated in the fluid element is the difference between the heat added and the heat leaving per unit time or

$$- \frac{\partial(\dot{w}\, c_p\, T)}{\partial x}\, dx + \frac{\partial\left[(k + \rho\, g\, c_p\, \epsilon_H')\, dA\, \frac{\partial T}{\partial x}\right]}{\partial x}\, dx$$

$$+ \frac{\partial\left[(k + \rho\, g\, c_p\, \epsilon_H'')\, dS\, \frac{\partial T}{\partial r}\right]}{\partial r}\, dr$$

Since steady state conditions are assumed, there is no heat accumulated. Therefore

$$\frac{\partial(\dot{w}\, c_p\, T)}{\partial x}\, dx - \frac{\partial\left[(k + \rho\, g\, c_p\, \epsilon_H')\, dA\, \frac{\partial T}{\partial x}\right]}{\partial x}\, dx$$

$$= \frac{\partial\left[(k + \rho\, g\, c_p\, \epsilon_H'')\, dS\, \frac{\partial T}{\partial r}\right]}{\partial r}\, dr$$

Now,

$$\dot{w} = u\, \rho\, g\, dA$$

Substituting for $\dot{w}$, dA, and dS,

$$2\pi r\, \frac{\partial(u\, \rho\, c_p\, T)}{\partial x}\, dx\, dr - 2\pi r\, \frac{\partial\left[(k + \rho\, g\, c_p\, \epsilon_H')\, \frac{\partial T}{\partial x}\right]}{\partial x}\, dx\, dr$$

$$= 2\pi \frac{\partial\left[r\, (k + \rho\, g\, c_p\, \epsilon_H'')\, \frac{\partial T}{\partial r}\right]}{\partial r}\, dx\, dr$$

Therefore,

$$\frac{\partial(u\, \rho\, g\, c_p\, T)}{\partial x} - \frac{\partial\left[(k + \rho\, g\, c_p\, \epsilon_H')\, \frac{\partial T}{\partial x}\right]}{\partial x}$$

$$= \frac{1}{r}\, \frac{\partial\left[r(k + \rho\, g\, c_p\, \epsilon_H'')\, \frac{\partial T}{\partial r}\right]}{\partial r} \qquad (12)$$

Since the fluid properties and channel flow area are

constant

$$u \rho g c_p \frac{\partial T}{\partial x} - (k + \rho g c_p \epsilon_H') \frac{\partial^2 T}{\partial x^2} - \frac{\partial (k + \rho g c_p \epsilon_H')}{\partial x} \frac{\partial T}{\partial x}$$

$$= (k + \rho g c_p \epsilon_H'') \frac{\partial^2 T}{\partial r^2} + \frac{\partial (k + \rho g c_p \epsilon_H'')}{\partial r} \frac{\partial T}{\partial r}$$

$$+ \frac{1}{r} (k + \rho g c_p \epsilon_H'') \frac{\partial T}{\partial r}$$

Finally,

$$u \rho g c_p \frac{\partial T}{\partial x} - (k + \rho g c_p \epsilon_H') \frac{\partial^2 T}{\partial x^2} - \rho g c_p \frac{\partial \epsilon_H'}{\partial x} \frac{\partial T}{\partial x}$$

$$= (k + \rho g c_p \epsilon_H'') \frac{\partial^2 T}{\partial r^2} + \rho g c_p \frac{\partial \epsilon_H''}{\partial r} \frac{\partial T}{\partial r}$$

$$+ \frac{1}{r} (k + \rho g c_p \epsilon_H'') \frac{\partial T}{\partial r} \qquad (13)$$

2. Expressions for the eddy conductivity

As a first step toward writing Eq. 13 in a more directly usuable form, the expressions referring to eddy conductivity will be restated in terms of known characteristics of the channel flow.

a. ϵ_H' The coefficient of eddy diffusivity for heat as it refers to turbulent mixing in the axial direction cannot be evaluated accurately if this evaluation is to be based on information published up to this time.

All complete channel analyses with which the author is familiar circumvent the necessity of evaluating ϵ_H' since they discard the entire axial conduction term, i. e.,

$(k + \rho g c_p \epsilon'_H) \partial^2 T / \partial x^2$, with a remark to this effect: "The second derivative of temperature with respect to x is generally negligible in comparison with the first." The validity of this assumption is seriously questioned.

If the term were to be included, a general relationship for ϵ'_H would be required. Determining this relationship and corroborating it experimentally would have to be accomplished by a scheme different from that followed in the determination of ϵ''_H, coefficient of radial turbulent conductivity. For the evaluations of ϵ''_H have been based on the effects of its counterpart, ϵ''_M, the coefficient of eddy diffusivity for momentum. The influence of ϵ''_M can be deduced from radial variations of the time-averaged axial velocity. No such profile exists of radial velocity versus axial location, since the time-averaged radial velocity is zero at every point in the channel.

In any case, no discussion of ϵ'_H was found in the literature, much less an attempted evaluation. However, the distinctive quality of turbulent flow is random motion of the fluid particles. Now, while "random" need not be a rigorously correct description, that is, a word implying statistical isotropy at any point, this description certainly implies some amount of turbulent fluctuation in all directions. Consequently, there is some amount of turbulent conduction in the axial direction. How this compares with turbulent conduction

in the radial direction is as yet an unsolved problem. There seem to be insufficient grounds even for a qualitative conclusion as to which is greater. However, it is unlikely that the mixing should occur so preferentially in the radial direction that only negligible components exist in the axial direction. For the sake of being able to apply Eq. 13 in its most general form and on the probability that the turbulent fluctuations have comparable components in the x and y directions, ϵ'_H is assumed equal to ϵ''_H.

b. $\partial \epsilon'_H / \partial x$ Since ϵ'_H is a function of the degree of turbulence, and, since the degree of turbulence is indicated by the Reynolds number once turbulent flow has developed, changes in ϵ'_H should be related to changes in Reynolds number. A fluid of constant properties has been postulated. For steady, fully developed turbulent flow of such a fluid through a channel of constant cross section, Reynolds number is unvarying at a given radius. Therefore, $\partial \epsilon'_H / \partial x$ may be reasonably equated to zero.

c. ϵ''_H The necessity for dividing the channel into two separate regions for purposes of analysis has been discussed previously. The coefficients of eddy conductivity for the two regions have been defined by Eqs. 4 and 6. By use of these equations and the relationships which follow, ϵ''_H will be expressed in terms of the dimensionless parameters, u^+ and y^+, which were previously defined.

As an intermediate step in Deissler's derivation of the velocity profile in the vicinity of the wall (4), the following derivative appears

$$\frac{du^+}{dy^+} = \frac{1}{1 + n^2 u^+ y^+}$$

The following derivative is found in the course of von Kármán's development for flow at a distance from the wall (12)

$$\frac{du^+}{dy^+} = \frac{1}{\kappa y^+}$$

Therefore, for the region close to the wall,

$$\frac{du}{dy} = \frac{\tau_w}{\mu} \frac{du^+}{dy^+} = \frac{\tau_w}{\mu(1 + n^2 u^+ y^+)}$$

Similarly, for flow in the main stream,

$$\frac{du}{dy} = \frac{\tau_w}{\mu} \frac{du^+}{dy^+} = \frac{\tau_w}{\kappa \mu y^+}$$

$$\frac{d^2u}{dy^2} = \frac{\tau_w \frac{\tau_w}{\rho}}{\frac{\mu^2}{\rho}} \frac{d^2u^+}{dy^{+2}} = \frac{-\tau_w \frac{\tau_w}{\rho}}{\kappa \frac{\mu^2}{\rho} (y^+)^2}$$

$$\frac{d^3u}{dy^3} = \frac{\tau_w^2}{\frac{\mu^3}{\rho}} \frac{d^3u^+}{dy^{+3}} = \frac{2 \tau_w^2}{\kappa \frac{\mu^3}{\rho} (y^+)^3}$$

In terms of the preceding relationships, ϵ_H'' near the wall can be expressed as

$$\epsilon_H'' = n^2 u y$$

$$\epsilon_H'' = \frac{n^2 \mu u^+ y^+}{\rho} \qquad (14)$$

Away from the wall, the applicable relationship is

$$\epsilon_H'' = \kappa^2 \frac{\left(\frac{du}{dy}\right)^3}{\left(\frac{d^2u}{dy^2}\right)^2} = \kappa^2 \frac{\frac{\tau_w^3}{\kappa^3 \mu^3 (y^+)^3}}{\frac{\tau_w^3 \rho^2}{\kappa^2 \rho \mu^4 (y^+)^4}}$$

$$\epsilon_H'' = \frac{\kappa \mu y^+}{\rho} \tag{15}$$

Equations 14 and 15 define ϵ_H' as well as ϵ_H'', since an equality between axial and radial turbulent mixing at a point has been assumed.

d. $\partial \epsilon_H''/\partial r$ To obtain this quantity, Eqs. 14 and 15 are differentiated.

Near the wall,

$$\frac{\partial \epsilon_H''}{\partial r} = n^2 (u + y \frac{du}{dy})$$

$$= n^2 \left[\sqrt{\frac{\tau_w}{\rho}}\, u^+ + \frac{\frac{\mu}{\rho}}{\sqrt{\frac{\tau_w}{\rho}}}\, y^+ \frac{\tau_w}{\mu (1 - n^2 u^+ y^+)} \right]$$

$$= n^2 \left[\sqrt{\frac{\tau_w}{\rho}}\, u^+ + \sqrt{\frac{\tau_w}{\rho}}\, \frac{y^+}{(1 + n^2 u^+ y^+)} \right]$$

$$\frac{\partial \epsilon_H''}{\partial r} = n^2 \sqrt{\frac{\tau_w}{\rho}} \left[u^+ + \frac{y^+}{1 + n^2 u^+ y^+} \right] \tag{16}$$

Away from the wall,

$$\frac{\partial \epsilon_H''}{\partial r} = \kappa^2 \left[\frac{3 \left(\frac{du}{dy}\right)^2 \left(\frac{d^2u}{dy^2}\right)^3 - 2 \left(\frac{du}{dy}\right)^3 \left(\frac{d^2u}{dy^2}\right) \left(\frac{d^3u}{dy^3}\right)}{\left(\frac{d^2u}{dy^2}\right)^4} \right]$$

$$= 3\kappa^2 \frac{\left(\frac{du}{dy}\right)^2}{\left(\frac{d^2u}{dy^2}\right)} - 2\kappa^2 \frac{\left(\frac{du}{dy}\right)^3 \left(\frac{d^3u}{dy^3}\right)}{\left(\frac{d^2u}{dy^2}\right)^3}$$

$$= 3\kappa^2 \frac{\frac{\tau_w^2}{\kappa^2 \mu^2 (y^+)^2}}{\frac{-\tau_w \sqrt{\frac{\tau_w}{\rho}}}{\kappa \frac{\mu^2}{\rho} (y^+)^2}} - 2\kappa^2 \frac{\frac{\tau_w^3}{\kappa^3 \mu^3 (y^+)^3} \frac{2\tau_w^2}{\kappa \frac{\mu^3}{\rho^3} (y^+)^3}}{\frac{-\frac{\tau_w^4}{\rho} \sqrt{\frac{\tau_w}{\rho}}}{\kappa^3 \frac{\mu^6}{\rho^3} (y^+)^6}}$$

$$= -3\kappa \frac{\tau_w}{\rho} + 4\kappa \sqrt{\frac{\tau_w}{\rho}}$$

$$\frac{\partial \epsilon_H''}{\partial r} = \kappa \sqrt{\frac{\tau_w}{\rho}} \qquad (17)$$

3. <u>The final equations</u>

Equation 13 will be rewritten, incorporating Eqs. 14 through 17 as well as two more dimensionless quantities, the Prandtl number, Pr, and the radius parameter, r^+, where

$$Pr = \frac{c_p \mu g}{k}$$

$$r^+ = \frac{\sqrt{\frac{\tau_w}{\rho}}}{\frac{\mu}{\rho}} r$$

Since $\partial \epsilon_H' / \partial x$ is zero, Eq. 13 can be written

$$\frac{\partial T}{\partial x} = \left(\frac{\mu}{u \rho Pr} + \frac{\epsilon_H'}{u}\right) \frac{\partial^2 T}{\partial x^2}$$

$$= \left(\frac{\mu}{u \rho Pr} + \frac{\epsilon''_H}{u} \right) \frac{\partial^2 T}{\partial r^2} + \frac{1}{u} \frac{\partial \epsilon''_H}{\partial r} \frac{\partial T}{\partial r}$$

$$+ \frac{1}{r} \left(\frac{\mu}{u \rho Pr} + \frac{\epsilon''_H}{u} \right) \frac{\partial T}{\partial r}$$

Since ϵ'_H is assumed the same as ϵ''_H,

$$\frac{\partial T}{\partial x} = \frac{1}{u} \left(\frac{\mu}{\rho Pr} + \epsilon''_H \right) \left(\frac{\partial^2 T}{\partial r^2} + \frac{\partial^2 T}{\partial x^2} \right)$$

$$+ \frac{1}{ru} \left(r \frac{\partial \epsilon''}{\partial r} + \frac{\mu}{\rho Pr} + \epsilon''_H \right) \frac{\partial T}{\partial r}$$

and, substituting r^+ and u^+ for r and u,

$$\frac{\partial T}{\partial x} = \frac{1}{\sqrt{\frac{\tau_w}{\rho}}\, u^+} \left(\frac{\mu}{\rho Pr} + \epsilon''_H \right) \left(\frac{\partial^2 T}{\partial r^2} + \frac{\partial^2 T}{\partial x^2} \right)$$

$$+ \frac{\rho}{\mu u^+ r^+} \left(\frac{\frac{\mu}{\rho}}{\sqrt{\frac{\tau_w}{\rho}}} r^+ \frac{\partial \epsilon''_H}{\partial r} + \frac{\mu}{\rho Pr} + \epsilon''_H \right) \frac{\partial T}{\partial r} \qquad (18)$$

A combination of Eq. 18 with Eqs. 14 and 16 yields the heat balance for flow near the walls.

$$\frac{\partial T}{\partial x} = \frac{1}{\sqrt{\frac{\tau_w}{\rho}}\, u^+} \left(\frac{\mu}{\rho Pr} + \frac{n^2 \mu u^+ y^+}{\rho} \right) \left(\frac{\partial^2 T}{\partial r^2} + \frac{\partial^2 T}{\partial x^2} \right)$$

$$+ \frac{\rho}{\mu u^+ r^+} \left[\frac{\frac{\mu}{\rho}}{\sqrt{\frac{\tau_w}{\rho}}} r^+ n^2 \sqrt{\frac{\tau_w}{\rho}} \left(u^+ + y^+ \frac{1}{1 + n^2 u^+ y^+} \right) \right.$$

$$\left. + \frac{n^2 \mu u^+ y^+}{\rho} + \frac{\mu}{\rho \, Pr} \right] \frac{\partial T}{\partial r}$$

$$\frac{\partial T}{\partial x} = \frac{\mu}{\rho \sqrt{\frac{\tau_w}{\rho}} u^+} \left(\frac{1}{Pr} + n^2 u^+ y^+ \right) \left(\frac{\partial^2 T}{\partial r^2} + \frac{\partial^2 T}{\partial x^2} \right)$$

$$+ \frac{n^2}{u^+ r^+} \left(u^+ r^+ + \frac{r^+ y^+}{1 + n^2 u^+ y^+} + \frac{1}{n^2 Pr} + u^+ y^+ \right) \frac{\partial T}{\partial r} \qquad (19)$$

A similar procedure can be followed in deriving a final form of the heat balance for the region at a distance from the wall. Thus,

$$\frac{\partial T}{\partial x} = \frac{1}{\sqrt{\frac{\tau_w}{\rho}} u^+} \left(\frac{\mu}{\rho \, Pr} + \frac{\kappa \mu y^+}{\rho} \right) \left(\frac{\partial^2 T}{\partial r^2} + \frac{\partial^2 T}{\partial x^2} \right)$$

$$+ \frac{\rho}{\mu u^+ r^+} \left(\frac{\frac{\mu}{\rho}}{\sqrt{\frac{\tau_w}{\rho}}} r^+ \kappa \sqrt{\frac{\tau_w}{\rho}} + \frac{\mu}{\rho \, Pr} + \frac{\kappa \mu y^+}{\rho} \right) \frac{\partial T}{\partial r}$$

$$\frac{\partial T}{\partial x} = \frac{\mu}{\rho \sqrt{\frac{\tau_w}{\rho}} u^+} \left(\frac{1}{Pr} + \kappa y^+ \right) \left(\frac{\partial^2 T}{\partial r^2} + \frac{\partial^2 T}{\partial x^2} \right)$$

$$+ \frac{\kappa}{u^+ r^+} \left(r^+ + \frac{1}{\kappa Pr} + y^+ \right) \frac{\partial T}{\partial r} \qquad (20)$$

Equations 19 and 20 are the governing relationships of the analysis. Equations 19 and 20, the velocity profile relationships, and the conditions of the physical problem (i. e., inlet temperature and pressure, weight rate of flow, heat flux as a function of axial station, properties of the fluid, and geometry of the system constitute nearly all the information needed to solve for the temperature distribution. The one quantity still lacking is shear stress at the walls. The following section is directed toward this end, i. e., determining τ_w.

The mode of applying Eqs. 19 and 20 may not be self-evident. As previously explained, the annulus is divided into two regions, inner wall, r_1, to the radius of maximum velocity, and outer wall, r_2, to r_{max}. In the outer region, y is equal to $(r_2 - r)$, and Eqs. 19 and 20 are functions of shear stress on the outer wall, τ_2; in the region between r_1 and r_{max}, y is $(r - r_1)$, and the equations are written with τ_w equal to τ_1.

C. Force Equations

As previously pointed out, the ultimate result of the following development will be a determination of the shear stresses at each of the annulus walls. The most elusive single unknown in a solution for the shear stresses is the radial location of maximum velocity, r_{max}. A scheme for determining r_{max} is derived, which is based essentially on a compatibility

of the velocity profile segments, begun as they are at opposite walls. At r_{max}, the quasi-independent determinations of velocity must yield the same value. Once r_{max} is established, the remainder of the derivation is accomplished by routine mathematical methods.

Since the velocity profile in a channel exhibits at the point of maximum velocity, at r_{max} in this case, a zero velocity gradient, and since $\tau = \rho \epsilon_M \, du/dr$, the shearing stress is zero at this point or rather over the surface $r = r_{max}$. On this basis, and by assuming constant pressure across any channel cross section, certain relationships for annulus wall shear stress can be derived.

For the annular fluid element of Figure 4 between r_1 and r_{max},

$$\left(p - p - \frac{dp}{dx}\,dx\right) \quad \pi\left(r_{max}^2 - r_1^2\right) = \tau_1 \, 2\pi r_1 dx$$

and

$$\tau_1 = -\frac{r_{max}^2 - r_1^2}{2r_1}\,\frac{dp}{dx} \tag{21}$$

Similarly solving for τ_2 as it influences the fluid volume from r_{max} to r_2,

$$\tau_2 = -\frac{r_2^2 - r_{max}^2}{2r_2}\,\frac{dp}{dx} \tag{22}$$

The dimensionless parameters earlier defined will be designated by subscript 1 if they refer to the region between the

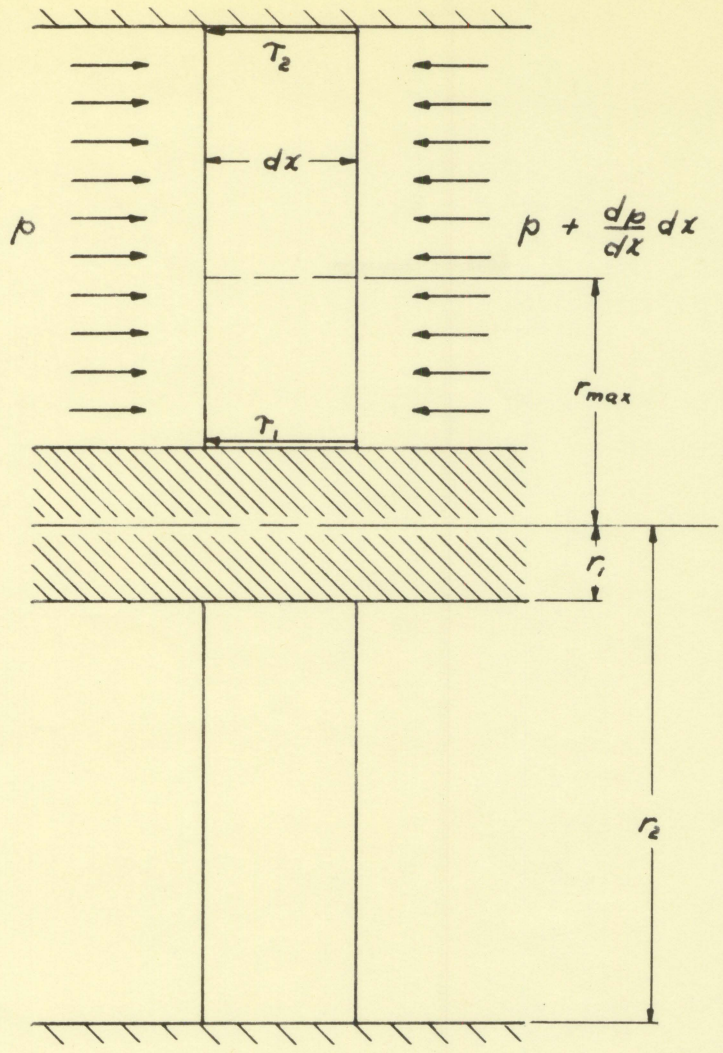

Figure 4. Stresses on an annular fluid element

core and r_{max}, by subscript 2, for the region between r_{max} and r_2. For example, y^+ insofar as it refers to y^+ in the inner region would be designated $y_1^+ = \frac{\sqrt{\tau_1/\rho}}{\mu/\rho} y_1$.

The iterative device next demonstrated is actually a logical development of the procedure outlined by Deissler and Taylor (6) for locating constant-velocity lines in eccentric annuli.

From Eqs. 21 and 22,

$$\frac{\tau_1}{\tau_2} = \frac{(r_{max}^2 - r_1^2)\, r_2}{(r_2^2 - r_{max}^2)\, r_1} \tag{23}$$

$$\sqrt{\frac{\tau_2}{\tau_1}} = \sqrt{\frac{(r_2^2 - r_{max}^2)\, r_1}{(r_{max}^2 - r_1^2)\, r_2}} \tag{24}$$

At r_{max}, u_1 equals u_2. Therefore,

$$\frac{u_{1max}^+}{u_{2max}^+} = \frac{u_{1max}}{\sqrt{\frac{\tau_1}{\rho}}} \cdot \frac{\sqrt{\frac{\tau_2}{\rho}}}{u_{2max}}$$

$$\frac{u_{1max}^+}{u_{2max}^+} = \sqrt{\frac{\tau_2}{\tau_1}} \tag{24a}$$

Moreover, in the generalized velocity profile, u^+ is a function of y^+, i. e.,

$$u_{1max}^+ = F\,(y_{1max}^+)$$

and

$$u_{2max}^+ = F\,(y_{2max}^+)$$

Define a type of Reynolds number,

$$R_1^+ = \frac{\sqrt{r_1 \frac{dp}{dx} \frac{1}{\rho}}}{\frac{\mu}{\rho}} r_1 \qquad (25)$$

By Eqs. 21 and 25,

$$\sqrt{\frac{(r_{max}^2 - r_1^2)}{2 r_1} \frac{1}{r_1}} R_1^+ = \sqrt{\frac{(r_{max}^2 - r_1^2)}{2 r_1} \frac{1}{r_1}} \frac{\sqrt{-r_1 \frac{dp}{dx} \frac{1}{\rho}}}{\frac{\mu}{\rho}} r_1$$

$$= \frac{\sqrt{\tau_1 \frac{1}{\rho}}}{\frac{\mu}{\rho}} r_1$$

Therefore,

$$y_{1max}^+ = \sqrt{\frac{(r_{max}^2 - r_1^2)}{2 r_1} \frac{1}{r_1}} R_1^+ \frac{y_{1max}}{r_1} \qquad (25a)$$

Now Eq. 26, the framework for the iterative procedure, can be set up. By Eqs. 24 and 24a, u_{1max}^+/u_{2max}^+ is expressed as a function of r_{max}. By Eqs. 25 and 25a, y_{1max}^+/y_{2max}^+ can be expressed as a function of r_{max} and an arbitrarily chosen value of R_1^+. Furthermore, the ratios of u_{max}^+ and y_{max}^+ are linked to each other by the universal velocity profile. The interdependence of the quantities referred to forms the basis for writing Eq. 26.

Equation 26 begins with the ratio of $\sqrt{\tau_1}$ to $\sqrt{\tau_2}$ as

determined by an estimated r_{max} (Eq. 24). The same r_{max}, when combined with the dimensionless number, R_1^+, defines y^+_{1max} and y^+_{2max} (Eq. 25a). Corresponding to each y^+_{max} is a u^+_{max} (from the universal velocity profile). Therefore, for a correct r_{max}, the ratio u^+_{1max}/u^+_{2max} as determined by the values of y^+_{max} is equal to the same ratio as determined by $\sqrt{\tau_2/\tau_1}$ (Eq. 24a). In other words, a correct estimate has been made for r_{max} when the first and last terms in Eq. 26 are equal.

Equation 26 is written

$$\sqrt{\frac{(r_2^2 - r_{max}^2)\, r_1}{(r_{max}^2 - r_1^2)\, r_2}} = \frac{F\left(\sqrt{\dfrac{r_2^2 - r_{max}^2}{2\, r_2 \over r_1}}\; R_1^+ \; \dfrac{y_{1max}}{r_1}\right)}{F\left(\sqrt{\dfrac{r_{max}^2 - r_1^2}{2\, r_1 \over r_1}}\; R_1^+ \; \dfrac{y_{2max}}{r_1}\right)}$$

$$= \frac{F(y^+_{1max})}{F(y^+_{2max})} = \frac{u^+_{1max}}{u^+_{2max}} \qquad (26)$$

The iteration procedure in detail is:

1. Assume a value for r_{max}. The only guide to this estimated value is that r_{max} is slightly closer to the annulus core wall than to the outer wall.

2. Substitute r_{max}, r_1, and r_2 into the left hand side of Eq. 26. This gives the ratio $\sqrt{\tau_2/\tau_1}$.

3. Choose an arbitrary value for R_1^+. This choice is

not critical, for an R_1^+ of 200 will give nearly the same ultimate result (the value of r_{max}) as an R_1^+ of 4000.

4. Solve for y_{1max}^+. The corresponding u_{1max}^+ can be deduced from von Kármán's formula, $u^+ = 2.78 \ln y^+ + 3.8$. A more involved integral equation applies for $y^+ < 26$. Should y_{1max}^+ or y_{2max}^+ fall below 26, use a larger R_1^+.

5. Solve in like manner for y_{2max}^+ and u_{2max}^+.

6. When the leftmost element (actually $\sqrt{\tau_2/\tau_1}$) and the rightmost element (u_{1max}^+/u_{2max}^+) of Eq. 26 are equal, r_{max} has been correctly estimated.

Return to Eq. 10, in which r_{max} and the known conditions of the problem are related to shear stress at the outer wall. This transcendental equation can be solved for τ_2 by an iterative method. Equation 23 can then be used to determine τ_1.

At this point, all quantities can be determined which are required in a solution of Eqs. 19 and 20, the equations which describe the temperature distribution in the fluid flowing through the annulus.

V. METHOD OF SOLUTION

A. Means of Calculation

The formal requirements, so to speak, of a solution have been fulfilled. What remains is a mathematical problem, the solution of a partial differential equation with variable coefficients.

One method of solution is presented here. The method proposed, that of finite differences, does not pretend to be an elegant one. However, the finite differences scheme does generally yield good results, and, in addition, does allow, to a moderate extent, for a choice of degree of accuracy. Additional terms of the Taylor series on which the method is based can be included and the incremental differences can be reduced to suit the calculator's needs. In short, the level of effort devoted to the calculations is more a measure of the accuracy of the method than the method itself. Mickley et al. (15) was consulted as a good engineering reference for determining a suitable method of solution.

The finite difference approach utilized consists in passing a plane through the axis of the annulus, and dividing the portion of this plane between the core and outer annulus wall into a grid of rectangles, each rectangle measuring Δx by Δr. Figure 5 shows this grid. Temperatures are solved for at each intersection point of the grid, and since the channel is axially symmetric in all respects, the solution in one

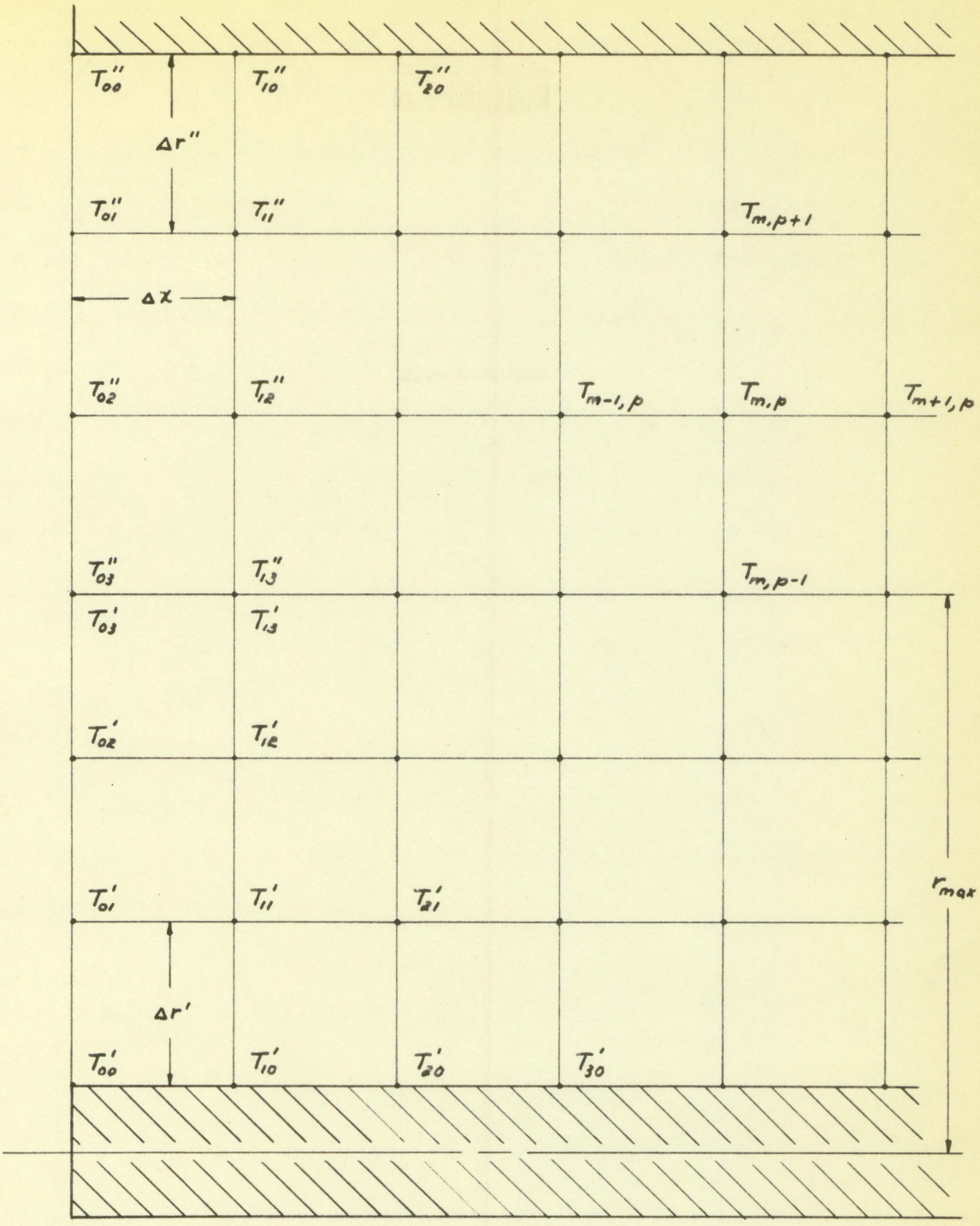

Figure 5. Annular channel temperature grid

plane describes the temperature distribution throughout the annulus. Individual temperatures are denoted by the subscripts m and p, where m refers to the appropriate x increment and p to the radial location. Note that the subscript numbering system begins at each wall and ends at the radius of maximum velocity, at least as far as the radial element, p, is concerned. This arrangement is required because the variable functions in the governing differential equations (Eqs. 19 and 20) depend not directly on radial distance from the axis but on distance from the respective walls. Further discussion of this temperature array will follow the transformation of Eqs. 19 and 20 into finite difference form. Equations 19 and 20 are of the general form

$$\frac{\partial T}{\partial x} = P(r)\left(\frac{\partial^2 T}{\partial x^2} + \frac{\partial^2 T}{\partial x^2}\right) + Q(r)\frac{\partial T}{\partial r}$$

The corresponding finite difference equation to the first approximation is

$$\frac{T_{m+1,p} - T_{m,p}}{\Delta x} = P(p\Delta r)\left[\frac{T_{m,p+1} - 2T_{m,p} + T_{m,p-1}}{(\Delta r)^2} + \frac{T_{m-1,p} - 2T_{m,p} + T_{m+1,p}}{(\Delta x)^2}\right] + Q(p\Delta r)\frac{T_{m,p+1} - T_{m,p}}{\Delta r}$$

Solving for $T_{m+1,p}$,

$$T_{m+1,p} = \frac{\Delta x}{\Delta x - P(p\Delta r)}\left\{\frac{P(p\Delta r)}{\Delta x}\left[(T_{m-1,p} - 2T_{m,p}\right.\right.$$

$$+ \left(\frac{\Delta x}{\Delta r}\right)^2 (T_{m,p+1} - 2T_{m,p} + T_{m,p-1})\Big]$$

$$+ Q(p\,\Delta r)\ \frac{\Delta x}{\Delta r}\ (T_{m,p+1} - T_{m,p}) + T_{m,p}\Big\} \qquad (27)$$

Although this is the general form of the equation, the functions P(r) and Q(r) refer to different relations, depending on whether y^+ is more or less than 26.

Evaluation of the functions P(r) and Q(r) at any radius is accomplished by the methods already detailed. The selection of increment size will be dictated by the needs of the particular problem. If computing equipment is available, increment size can be reduced until no appreciable increase in accuracy is effected. Another criterion of increment size is one of convenience; if the distance from the wall to the radius of maximum velocity is an exact multiple of Δr, and if the channel length is an exact multiple of Δx, the necessity of interpolation is avoided.

The final difficulty lies in arriving at some initial temperature values from which further calculation can proceed. This leads to a discussion of the problem's boundary conditions, a matter not yet explicitly discussed.

One of the known conditions of the problem is the variation of heat flux with axial distance. This heat flux is assumed known in terms of the specific rate of heat flow, q(BTU per hour per square foot), for all x. At the

core wall eddy conductivity vanishes, so that molecular conductivity is the only mode of heat transport that need be considered. At r_1, then, the following equation is valid:

$$(q)_{r=r_1} = q_1 = -k \frac{\partial T}{\partial r} \tag{28}$$

To adapt Eq. 28 to a form usable in the general scheme of solution, this differential equation can be written

$$q_1 = -k \frac{T_{r_1} + \Delta r - T_{r_1}}{\Delta r}$$

or

$$q_1 = k \frac{T_{m,o} - T_{m,1}}{\Delta r} \tag{29}$$

The assignment of initial values in a finite differences solution typically entails some amount of compromise. One approach is to equate temperatures T_{01}, T_{02}, ..., $T_{0,p}$ to the inlet temperature of the fluid. A possible assumption for the row of temperatures immediately preceding the channel entrance is to assume that these temperatures also are at inlet bulk temperature. Thus, $T_{-1,1}$, $T_{-1,2}$, ..., $T_{-1,p}$ are also known. The temperatures T_{11}, T_{12}, ..., $T_{1,p}$ can now be evaluated by applying Eq. 27. Equation 29 is solved with a new q_1, and with T_{11} to find T_{10}. The process is repeated until the entire temperature grid between r_1 and r_{max} is completed.

Development of the temperature grid between r_{max} and r_2 represents a simpler process. In this region, the known

values are all the temperatures at x = 0 (the inlet temperature) and all temperatures at $r = r_{max}$ (as solved for in the r_1 to r_{max} calculations). Only the values at $r = r_2$ present any difficulty. Since the outer wall of the annulus is considered perfectly insulated $\partial T / \partial r = 0$ at that point. Following the same line of reasoning as that behind the formulation of Eq. 29, the temperature at $r = r_2$ is the same as that at $r = (r_2 - \Delta r)$. The calculations for the region between r_{max} and r_2 complete the procedure to adequately describe the temperature distribution in the system. The preceding is a broad outline of the method of applying the finite difference equations. Some variations on this method are described in greater detail in the following section.

A commonly desired quantity in heat transfer problems similar to the one just solved is the bulk or completely-mixed temperature of the fluid. This quantity is solved for from the known temperature and velocity distributions. The defining equation for bulk temperature in an annular passage is

$$\dot{w}\, c_p\, T_{bulk} = \int_A T\, u\, \rho\, g\, c_p\, dA$$

where

$$A = \pi(r_2^2 - r_1^2)$$

For a fluid of constant properties, the equation can be simplified and transformed into difference form as

$$(T_{bulk})_x = \frac{2\Delta r \sum_{r_i=r_1}^{r_2} T(x,r_i)\ u(r_i)\ r_i}{u_m(r_2^2 - r_1^2)}$$

B. Example

For the purpose of applying the derived equations to the solution of a typical problem, the following physical situation was assumed.

A concentric annulus with heated core and perfectly insulated outer wall is cooled by air flowing with a mean velocity of 100 fps. The dimensions of the annulus are:

Core radius, $r_1 = 0.2500$ ft

Outer radius, $r_2 = 0.3333$ ft

A section of the channel 2.000 ft in length was chosen for analysis. The annulus core over this length is heated according to the axial heat flux distribution shown in Figure 6.

The air flow is assumed fully turbulent when it enters the length of channel under analysis. Entering air is at a bulk temperature of 400°F and under a pressure of 5 atmospheres.

This information and a compilation of the properties of air, such as that presented by Eckert and Drake (8, p. 274), are sufficient data for beginning a solution to the problem.

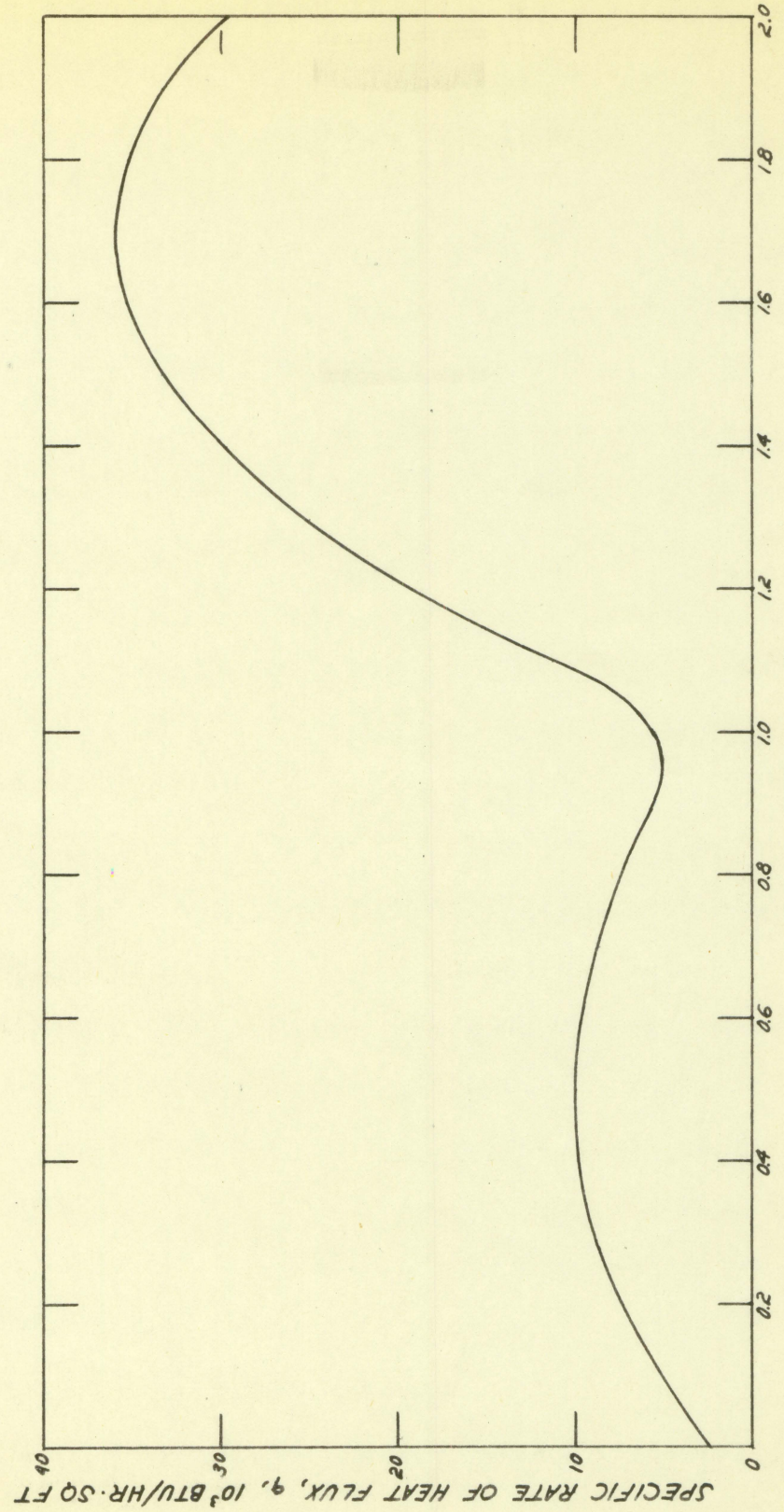

Figure 6. Axial heat flux distribution, example

By an iterative solution to Eq. 26, r_{max} is found to be 0.2895 ft. By an iterative solution to Eq. 10, τ_2 is found to be 0.1357 lb/sq ft. Equation 23 gives a τ_1 of 0.1413 lb/sq ft.

There follows a brief description of the customary approximate solution for wall temperatures and fluid bulk temperatures. The purpose of these calculations is to provide a general comparison with the results of the present analysis.

The change in bulk temperature of the fluid is determined by assuming slug flow of the air and by numerically integrating the heat supplied to the fluid over the length of the channel. Axial conduction within the fluid is neglected. By calculations based on this method, a fluid bulk temperature rise of 17.69 Fahrenheit degrees is predicted. A like integration of the heat transmitted to the fluid up to a given point in the channel yields the increase in bulk temperature between the inlet and that point in the channel.

In addition to the fluid bulk temperature, it is important to know the surface temperature of the heated wall. To find this quantity at any axial location, the local bulk temperature value is used in conjunction with the film heat transfer coefficient, h, and the specific rate of heat flux, q_1. By definition,

$$q_1 = h(T_w - T_{bulk}) \tag{31}$$

According to a widely accepted expression based on heat

transfer experimental results,

$$h = \frac{k}{2(r_2 - r_1)} \; 0.023 \; (Re)^{0.8}(Pr)^{0.4}$$

See Hall (10, p. 13). The film heat transfer coefficient for this example was found to be 49.42 BTU/(hr)(sq ft)(^{o}F). Wall temperature is calculated by rearranging Eq. 31 to read

$$T = \frac{q_1}{h} + T_{bulk}$$

Results of the wall temperature calculations are presented in graphical form later in this section. These temperatures, calculated from the bulk temperature and the heat transfer coefficient, are considered reasonably correct values with which final results of the present analysis can be compared, at least in an approximate manner.

It was considered desirable to devise a method of solution that would fulfill the following two criteria without compromising reasonably accurate results. First, maximum possible simplification of the calculations was sought. Second, the difference equations were to be written with large enough increments to allow for a solution by desk calculator.

The principal assumptions of the first attempt at a solution were that flow in the region between r_1 and $y^+ = 26$ was laminar and that $\partial^2 T / \partial x^2$ was negligible (a common simplification in solving this type of problem). The assumption of laminar flow from the wall to y^+ of 26 was based on the shallowness of this region; $y = 0.0004472$ ft at $y^+ = 26$. As a

reasonably acceptable starting condition for the calculations, all temperatures at the entrance from $y^+ = 26$ to the insulated wall were considered to be 400°F. By a difference equation of the form of Eq. 29, the temperature at the wall was found from k, the q_1 at $x = 0$, and the distance between $y^+ = 0$ and $y^+ = 26$. Since a thin layer of laminar flow was assumed, the temperature at $y^+ = 13$ can be found from the temperature at $y^+ = 0$, the temperature at $y^+ = 26$, and the assumption of a linear temperature variation between the two points. If $2\Delta r = 0.0004472$ ft (y at $y^+ = 26$), temperatures T_{00}, T_{01}, and T_{02} are known (refer to Figure 5). Since $\partial^2 T/\partial x^2$ is assumed negligible, Eq. 27 is applied without the term (in difference form), $P(r)\ \partial^2 T/\partial x^2$. When Eq. 27 is thus simplified, temperatures T_{00}, T_{01}, and T_{02} provide the required number of known quantities for T_{11} to be calculated. When the assumption of a purely laminar region in the vicinity of the wall is once more utilized, T_{12} and T_{10} are found from the conductive equation, Eq. 29. By a repetition of the procedure just outlined, all temperatures at $y^+ = 0$, $y^+ = 13$, and $y^+ = 26$ are calculated.

When the method was followed in the manner described, the rise in wall temperature over the first tenth of the channel was calculated to be 793.8°F. By the very nature of this approach, the temperatures at $y^+ = 26$ underwent exactly the same unexpectedly large increase. There seems to be a logical explanation for this large axial temperature rise. Since there

exists some amount of turbulence even when y^+ is less than 26, the temperature differences between two radial points near the wall are less than the differences indicated by the laminar assumption. Other things being equal (i. e., flow conditions and fluid properties), the temperature difference is proportional to q_1. Consequently, solution of Eq. 27 with an unrealistically high temperature difference near the wall is essentially a solution for a wall heat flux which is higher than the actual case. Under such circumstances, an excessive temperature rise is understandable.

This apparent discrepancy led to a closer scrutiny of the equations as originally derived, this scrutiny extending especially to the simplifying assumptions that were made. Two modifications which seemed appropriate were incorporated into a second attempt at solving the problem.

First, the term $\partial^2 T / \partial x^2$, generally discarded in this sort of derivation, was included in the heat balance. Inclusion of this quantity necessitated evaluating its coefficient, $(k + \rho g c_p \epsilon'_H)$. While the intermolecular conductivity, k, is a known property of the fluid, no guidance was found toward a quantitative determination of ϵ'_H. For the reasons presented in Section IV, ϵ'_H was assumed equal to ϵ''_H.

The second important modification was to abandon the assumption of a linear temperature versus distance from the wall relationship from $y^+ = 0$ to $y^+ = 26$. The small thickness (0.0004472 ft) of this region is deceptive in so far as severe,

non-linear variations in temperature occur between its limits. One means of solution which is not dependent on the linear temperature distribution assumption over a Δy^+ of 26 is to drastically reduce the increment size, Δr; for Eq. 29 can be directly applied with good accuracy if the radial increment is made small enough. However, difference equations with increments sufficiently small for a reliable direct application of Eq. 29 involve far too many temperature grid node points to permit a feasible solution by desk calculator.

An alternate means of avoiding the linear temperature distribution simplification, and a means which does not involve reduced distance increments is to refer to the universal temperature profile.

The universal temperature profile or generalized temperature distribution is a plot of T^+ versus y^+ where

$$T^+ = \frac{(T_w - T)\, g\, c_p\, \tau_w}{q_w \sqrt{\frac{\tau_w}{\rho}}} \qquad (32)$$

Whereas the universal velocity profile is, in the final analysis, the result of integrating Eq. 1 and expressing the results in terms of the dimensionless parameters, u^+ and y^+, the generalized temperature distribution is the integrated result of Eq. 2. It can be seen from Eqs. 1 and 2, and from the definitions of the dimensionless parameters, that, for a fluid of Prandtl number equal to one, the generalized velocity and temperature distributions are identical. Deissler and Taylor

(6, p. 27) show the temperature distribution for air. By means of this curve, the temperature difference between the heated wall and a point in the channel can be determined if heat flux from the wall and y^+ of the point are known. This temperature difference is expected to be more realistic than that derived from the assumption of a layer of laminar flow from the wall to $y^+ = 26$.

It must be noted that the generalized temperature distribution is intended only for a fully developed temperature profile, one which is constant along the length of the channel, and an axial variation in q_w is not compatible with this restriction. However, in spite of this incompatibility, use of the profile curve was attempted in the hope that a reasonably accurate description of the temperature distribution near the wall would be provided.

The second approach begins, like the first attempt, with an assumption that inlet temperatures from $y^+ = 26$ to r_2 are $400^\circ F$. By means of the plot of the generalized temperature distribution referred to in the previous paragraph, T^+ for $y^+ = 13$ and for $y^+ = 26$ can be determined. By Eq. 32 and q_1 at $x = 0$, temperatures at $y^+ = 0$ (T_{00}) and at $y^+ = 13$ (T_{01}) can be found, if the temperature at $y^+ = 26$ (T_{02}) is known (assumed at $400^\circ F$ in this case). Since $\partial^2 T / \partial x^2$ is taken into account, an additional assumption is required, this assumption referring to temperatures before the channel inlet. Let all temperatures at $x < 0$ be $400^\circ F$. This last assumption gives a

value for $T_{-1,1}$, the temperature just preceding the channel entrance, that is, at $x = -\Delta x$. Since $\partial^2 T / \partial x^2$ is included in this attempt, Eq. 27 was used in its entirety. All quantities necessary to solve for $T_{m+1,p}$, T_{11} in this case, are known. From q_1 at $x = \Delta x$ and from Eq. 32, T_{12} and T_{10} were found from T_{11}. T_{21} was found from a substitution of T_{01}, T_{10}, T_{11}, and T_{12} into Eq. 27. The procedure was repeated until temperatures were defined at y^+ of 0, 13, and 26 for the entire channel.

As far as calculations in the main stream region are concerned, they begin at y^+ of 26, where all temperatures are known from the work just done. From these known temperatures and from the assumptions made for the temperature before and at $x = 0$, it is apparent that Eq. 27 can be applied to find temperatures throughout the main flow region between r_1 and r_{max}.

The calculations between r_{max} and r_2 are based on an axial line of known temperatures (at r_{max}) and the temperature assumptions for $x = 0$ and $x < 0$. In the last temperature increment before r_2, Eq. 29 is applied. Since q_w is zero at an insulated wall, Eq. 29 dictates equal temperatures at the outer wall and at the first radial position away from it.

The whole procedure just outlined seemed defective in some respect(s), because unrealistically high temperature increments were again encountered. Although additional

corrective modifications were indicated, calculations were continued to complete the entire temperature grid. In spite of excessive axial temperature increments, it was believed that the completed grid would reveal anything abnormal in the manner in which radial temperature profiles developed. Figure 7 shows the temperature grid over the first tenth (0.2 ft) of the channel length analyzed. This first tenth is divided into small increments so as to quickly close the "wedge" of equal temperatures that result from this particular method of beginning the calculations. Note that the temperatures in this figure and in Figure 8 are not shown directly, but as $(T - 400)^{\circ}F$, as though inlet bulk temperature were $0^{\circ}F$. The purpose for representing the temperatures in this manner was to show more clearly the frequently small temperature increases from point to point in the grid. Figure 8 covers the entire channel. While the temperature rise in the x direction appears entirely too great, and the final bulk temperature far in excess of the expected 418°, the temperature gradient in the radial direction seems to follow a reasonable pattern.

The third approach toward a solution differs from the second approach in the manner in which the derivatives $\partial T/\partial r$ and $\partial^2 T/\partial r^2$ were evaluated. It was assumed that the calculations just discussed were being adversely affected by incorrect values for these derivatives. The finite difference expressions for $\partial T/\partial r$ and $\partial^2 T/\partial r^2$ which include temperatures at y^+ of 0, 13, and 26 seem to be poor representations

Figure 7. Temperature distribution, (T-400)°F, first tenth of channel

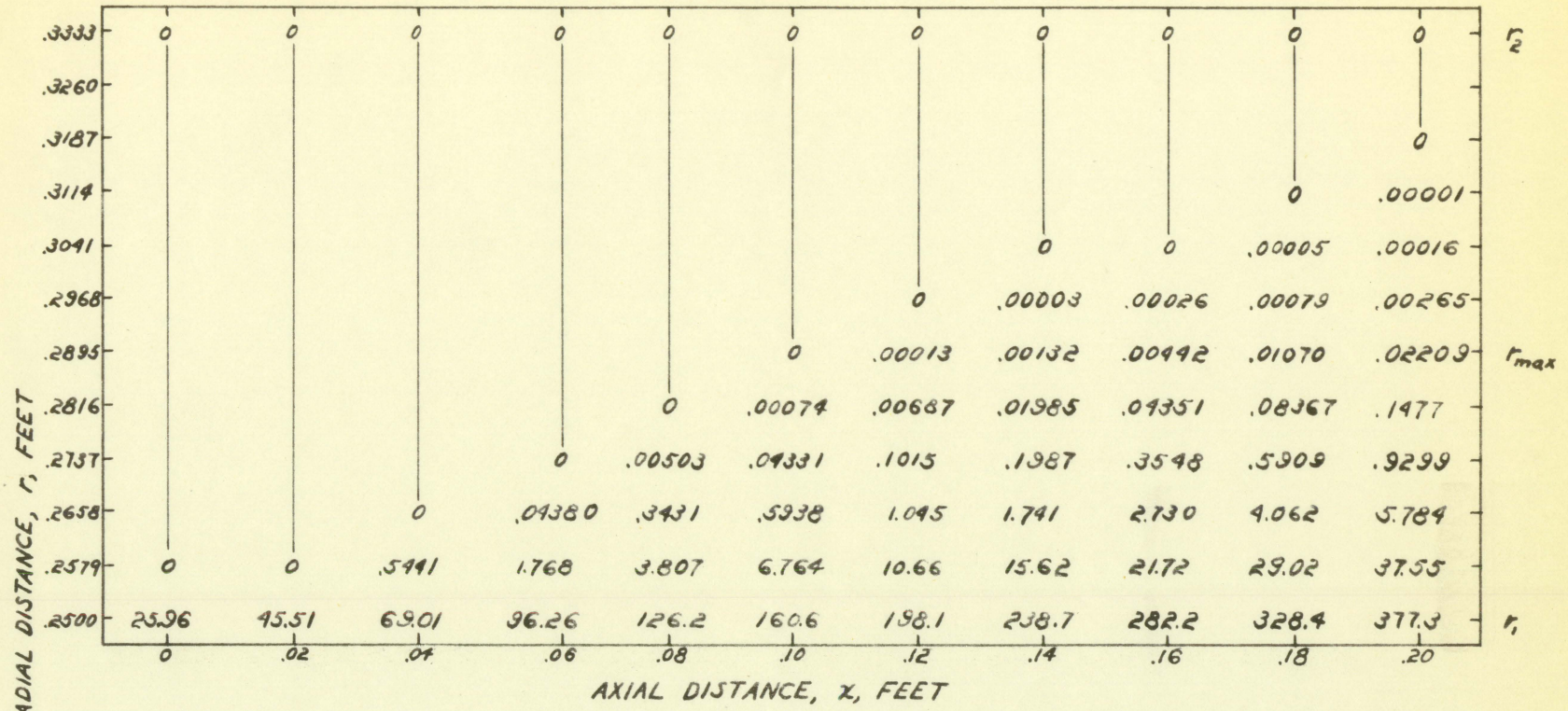

ENTIRE CHANNEL

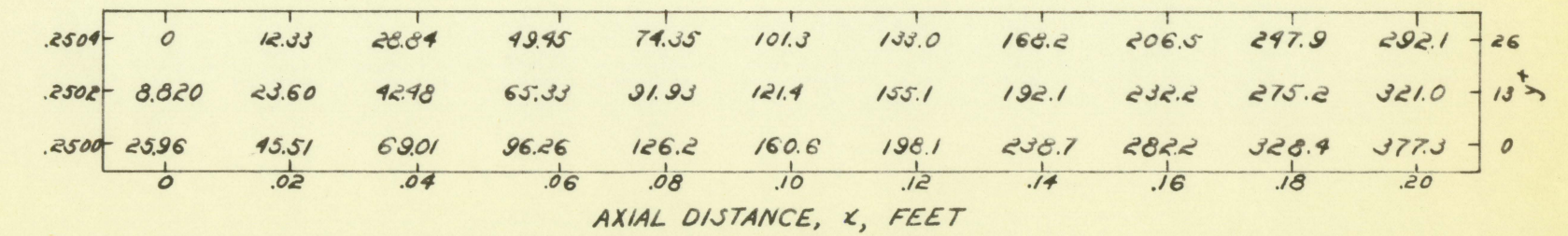

FROM CORE WALL TO $y^+ = 26$

Figure 8. Temperature distribution, (T-400)°F, entire channel

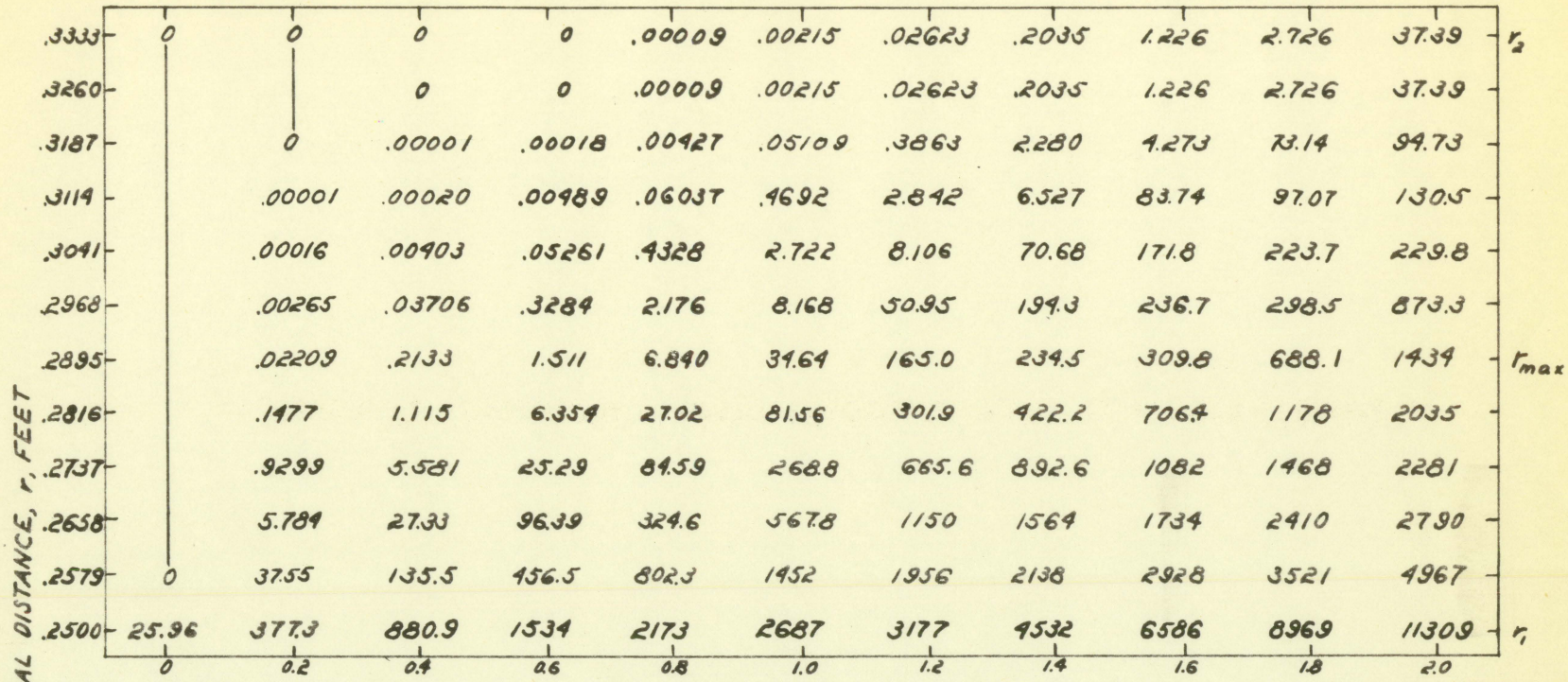

ENTIRE CHANNEL

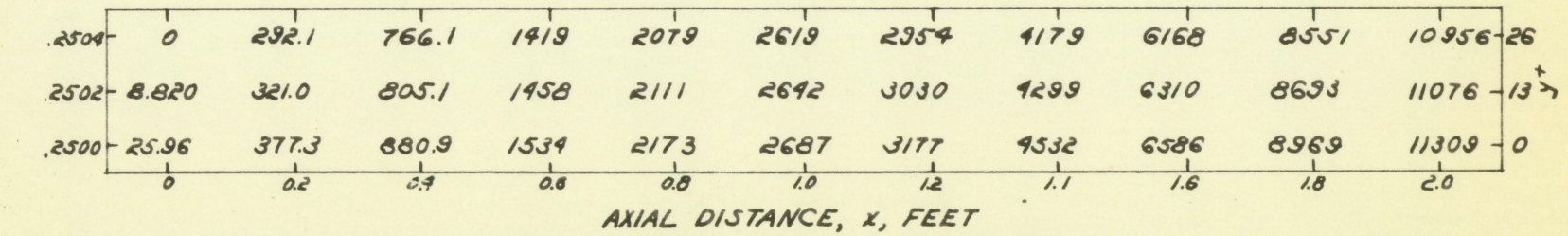

FROM CORE WALL TO $y^+ = 26$

of the derivatives themselves. This is because the change of the radial temperature gradient is so rapid in the region near the wall that a Δy^+ of 13 corresponds to a gross radial increment, Δr. To avoid decreasing increment size (for the reason presented earlier), while still improving accuracy in expressing the derivatives of temperature with respect to radial distance, Eq. 2 was used in the form

$$\frac{\partial T}{\partial r} = \frac{-q_w}{(k + \rho g c_p \epsilon_H)}$$

The second derivative was found by differentiating this equation. Equations 4 and 6 define ϵ_H in the two regions of flow. Since these four relationships make it possible to evaluate the derivatives exactly for a given y^+ and q_w, $\partial T/\partial r$ and $\partial^2 T/\partial r^2$ can be substituted into the equations directly, rather than in difference form. Consequently, Eq. 27 can be rewritten

$$T_{m+1,p} = \frac{\Delta x}{\Delta x - P(p\Delta r)} \left\{ \frac{P(p\Delta r)}{\Delta x} \left[(T_{m-1,p} - 2T_{m,p}) + (\Delta x)^2 \frac{\partial^2 T}{\partial r^2} \right] + Q(p\Delta r)\, \Delta x \frac{\partial T}{\partial r} + T_{m,p} \right\} \qquad (33)$$

Although the third attempt differs from the first in that a slightly different equation is used, the same starting assumptions are made. On the basis of a known $T_{-1,1}$, T_{01}, $(\partial T/\partial r)_{y^+ = 13}$, and $(\partial^2 T/\partial r^2)_{y^+ = 13}$, T_{11} is calculated by

Eq. 33. By repeated use of this equation, all temperatures at y^+ of 13 can be found. Wall temperatures along the channel length can be found from the line of temperatures at $y^+ = 13$ and Eq. 32.

Although results from this mode of solution showed improvement over previous attempts, higher temperatures than would be expected developed once more as the calculations proceeded along the channel. (The results of an approximate calculation as outlined by Eckert and Drake (8, pp. 124-125) showed a total bulk temperature rise of some 400° over the inlet bulk temperature.)

Figure 9 compares wall temperatures as calculated according to the second and third solution attempts with results of the usual approximate solution. Curve 1 is the wall temperature as derived from the conventional method of an approximate solution, wherein the bulk temperature and film heat transfer coefficient concepts are applied. Curve 2 is a plot of the results according to the second approach, in which Eq. 27 was used completely in difference form, and the universal temperature profile was used to determine temperature differences in the region close to the wall. Curve 3 shows wall temperatures as calculated by the last scheme described, in which the derivatives of temperature with respect to radial distance were substituted directly into the modified difference equation, Eq. 33.

Figure 9. Core wall temperatures as calculated by three methods

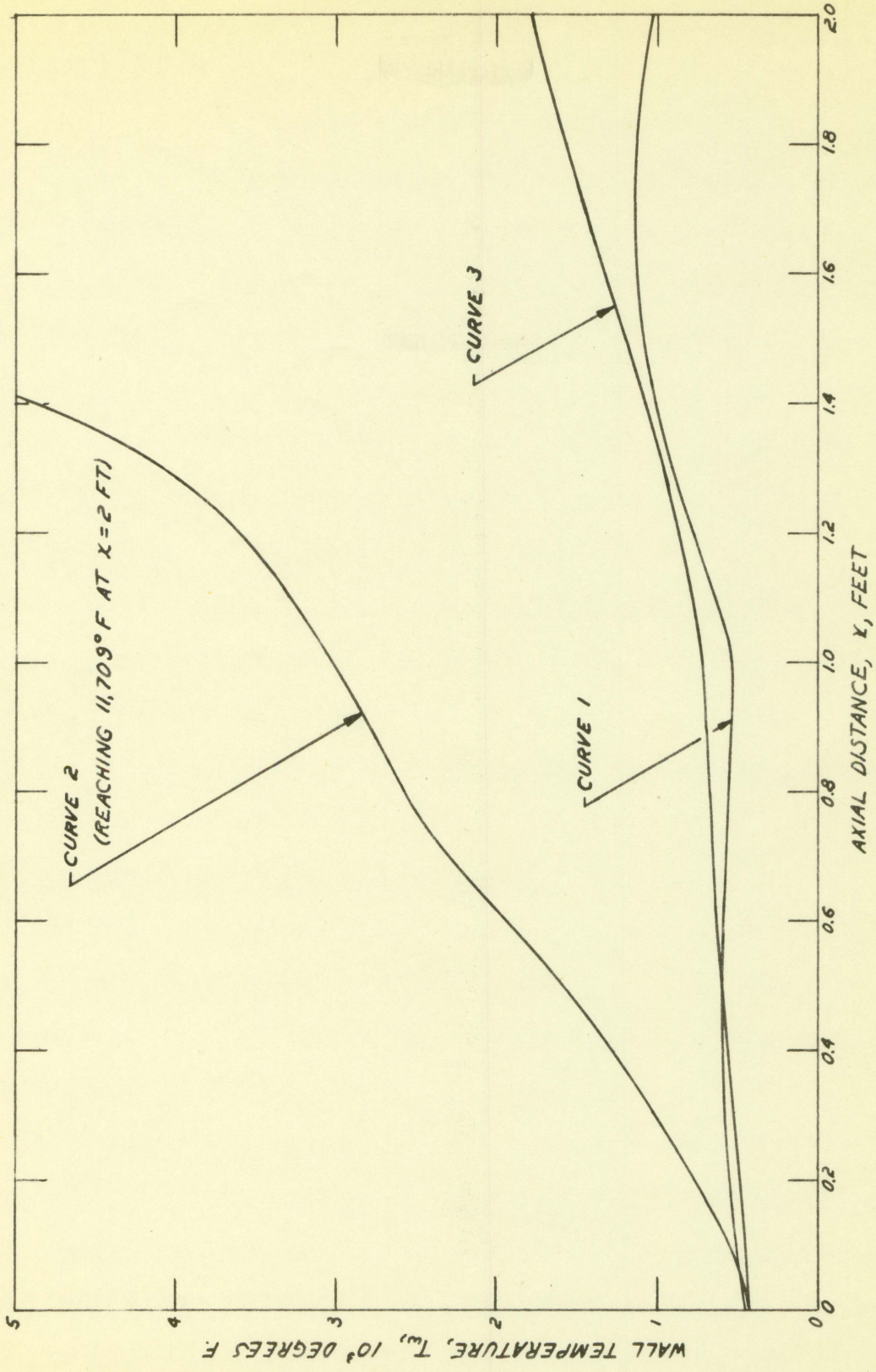
WALL TEMPERATURE, T_w, 10^3 DEGREES F
AXIAL DISTANCE, x, FEET
CURVE 1
CURVE 2
(REACHING 11,709° F AT x = 2 FT)
CURVE 3
0
0.2
0.4
0.6
0.8
1.0
1.2
1.4
1.6
1.8
2.0
1
2
3
4
5

VI. CONCLUSIONS

A. Possible Sources of Error

While no exact correlation was expected between the results of the present analysis and the conventional means to an approximate solution, the broad divergence between the two sets of results indicates a discrepancy either in the derivation presented in this paper, in the assumptions on which that derivation was based, or in the method of solution. The various possible sources of error will be considered in turn.

1. Correctness of the derivation

Although Eqs. 19 and 20 are products of considerable mathematical manipulation, numerous reviews of the derivation have only corroborated their mathematical correctness. The equations were checked in particular for dimensional correctness throughout the development.

2. Validity of original assumptions

The only original assumption that resulted in the omission of a term was the assumption that $\partial \epsilon'_H / \partial x$ was zero. The reasons, as given earlier, seem adequate to justify this omission.

The only other original assumption was that of setting axial eddy conductivity equal to radial eddy conductivity. If this assumption were influencing the results adversely, it would have to be changed in the direction of making the axial eddy conductivity much greater than the radial component.

3. Validity of non-original material used

There is the possibility, though not a strong one, that the development, in being based on the results of several independent efforts, compounds their assumptions and/or errors to its own detriment. Two individual assumptions may well have a bearing on the results.

The scheme for determining wall shear stresses (Eq. 10) is the item in the derivation least corroborated by experimental results. It can be seen from the equations that a serious error in calculating this quantity has far-reaching effects on the results.

A common but much controverted assumption is that of equating eddy viscosity and eddy conductivity (the Prandtl analogy). The validity of this assumption was referred to briefly early in this paper. When specifically investigated, ϵ_H is found to be always greater than ϵ_M, slightly greater near a solid boundary and becoming almost twice as large in the main stream. The inequality of the two turbulent effects is rather an accepted fact. However, no effective correlations have been made by which the ratio between the two can be determined for various points in a given situation even though flow conditions can be well defined. In other words, only specific measurements for specific cases are available. The influence of the value of ϵ_H is extremely important in the present development and in any turbulent heat transfer analysis.

4. Validity of the method of solution

Use of the generalized temperature distribution in conjunction with the boundary conditions and finite difference equations seems of questionable validity. For, just as the universal velocity profile is based on fully developed turbulent flow and a fully developed, very nearly constant velocity profile, the generalized temperature distribution is intended only for situations in which temperature profiles are nearly constant with respect to axial position. This is not the case when q_w is allowed to vary arbitrarily with axial location. Moreover, the generalized temperature distribution is based on the just discussed assumption of equal coefficients of eddy conductivity and eddy viscosity. Therefore, it is considered important that the solution be accomplished without dependence on the generalized temperature distribution.

It is clearly an error to assume laminar flow for the entire region between r_1 and y^+ of 26, as was done in the first attempt at a numerical solution. However, the basic conduction equation, Eq. 29, must be valid over some small radial increment next to the heated wall. A y^+ increment of 2 or 3 is considered a suitable dimension for this increment. For the specific example for which a solution was attempted, a y^+ of 3 corresponds to a Δr of 0.00003440 ft. It is apparent that increments of this size require a numerical solution beyond the range of the desk calculator and in the realm of a digital computer.

One final aspect of the mode of solution warrants discussion. The finite difference approach as outlined in the previous section requires that the radial temperature distribution be known or assumed at $x = 0$ as well as at $x = -\Delta x$. It is considered advisable to devise an approach whereby the number of assumed temperatures is halved, that is, only the profile at $x = 0$ is supplied for a solution to the problem. However, knowing temperatures only at $x = 0$ provides insufficient information to begin a solution by the methods thus far discussed. For Eq. 27 involves temperatures T_{01}(known), T_{10}, T_{11}, T_{12}, and T_{21}. Equation 29 links temperatures T_{10} and T_{11} by a known relationship. The availability of just two equations, while the unknown temperatures number four, prevents the solution for the first unknown temperature, the temperature which must be substituted into subsequent equations to begin a progressive solution for all temperatures in the grid. No progressive step-by-step solution is possible under the conditions as described.

B. Solution by Simultaneous Equations

An alternate method of solution is that of solving a set of simultaneous equations covering the entire grid. If the temperature grid is divided into p divisions in the radial direction, there are, for each column in the grid, $p + 1$ unknown temperatures. If the grid has m axial divisions, there are m rows of unknown temperatures if all temperatures at

$x = 0$ are known. Therefore, the total number of unknowns in the system is $m(p + 1)$. The number of finite difference equations of the form of Eq. 27 that can be written for the interior nodes of each column of the grid is $p - 1$. Equation 29 can be applied at each wall for all axial stations. This increases the number of equations per column to $p + 1$. With the column of temperatures at $x = 0$ either known or assumed, and with all columns from Δx to $(m - 1)\Delta x$ provided with as many simultaneous equations as there are unknowns, only the last column offers any difficulty. Equation 29 applies at top and bottom of this column, just as it did for earlier columns. However, finite difference equations cannot be written about the interior points in this column (there are $p - 1$), since these equations each include one temperature beyond the channel. Some assumptions regarding the temperatures between $r = (r_1 + \Delta r)$ and $r = (r_2 - \Delta r)$ at the cross section Δx feet beyond the channel are demanded. These assumptions can be made to match the exit conditions of the particular problem being solved. One approach that seems reasonable for most expected physical situations (especially when extremely small longitudinal increments are used) is to assume equal temperatures at $m\Delta x$ and at $(m + 1)\Delta x$ for a given radius. This assumption supplies $p - 1$ equations, the number of additional relationships needed to match the number of unknown temperatures. Use of an electronic computer would be indispensable for this method of solution, since the number of simultaneous

equations would be considerable for even moderate radial and axial increments.

The computer solution by simultaneous equations has the following advantages.

1. Small enough increments can be employed so that no use need be made of the generalized temperature distribution, and the boundary condition of known heat flux can be applied directly and validly through Eq. 29.

2. Small enough increments can be employed so that the difference forms of $\partial T/\partial r$ and $\partial^2 T/\partial r^2$ can accurately represent these derivatives even in extremely sensitive regions.

3. Very little complexity would be added to the solution if q at the wall hitherto considered insulated were allowed to have a value, even if this value were allowed to vary axially as it does at the core wall.

4. In a step-by-step solution, the influence of the heat flux from each wall at a given axial location does not extend entirely across the channel until a number of increments, Δx, downstream. In a solution by simultaneous equations, however, the heat flux from each wall at a given axial station affects the entire temperature profile at that station.

While a solution by simultaneous equations shows good promise, it is principally an improvement in the mathematics of applying Eqs. 19 and 20. For improved reliability of the heat transfer equations proper, additional analysis and

experiment must yield more accurate, generalized relationships for eddy conductivity, both in a radial and an axial direction.

VII. SUMMARY

A. Nature of Derivation

The derivation presented in this thesis yields the two governing equations for heat transfer to a turbulent fluid in forced convection through an annulus. The derivation draws upon the best information published up to this time on turbulent channel flow, on turbulent heat transfer, and on the problems peculiar to annular geometry. All material used is corroborated to some extent by experimental data. Without exception, the relationships refer to conditions over the cross section of a channel of uniform axial properties. The effort was directed at validly adapting these relationships to a situation of axially varying heat flux, a situation frequently encountered in engineering applications.

B. Results of Sample Calculations

The resulting differential equations were applied to a rather typical engineering problem. A finite difference scheme was proposed whereby a solution could be accomplished by desk calculator in a reasonable amount of calculation time. The calculations, even after several refinements, consistently predicted fluid temperature increments far in excess of expected values. Present lack of an adequate quantitative description of the turbulent mixing phenomenon as it affects heat transport is conjectured to be at least a partial reason

for the unexpected results. It is felt that an even greater influence is exerted by the general approach to solving the equations. Although the same set of finite difference equations is to be retained, certain modifications are recommended which would necessitate the use of an electronic computer. The most important change would be a drastic decrease in the size of the increments appearing in the difference equations.

C. Alternate Means of Solution

As stated above, the simpler method of solution first proposed seems deficient. Consequently, a computer solution by simultaneous equations is advocated. The simultaneous solution seems to offer some advantage. However, the principal benefit of employing an electronic computer is the possibility of reduced increment size. The relationships involved are rather straight-forward and no unusual obstacles to programming the problem for machine computation are anticipated.

D. Contributions of Present Analysis

The contributions of the paper to the field of convective heat transfer to a turbulently flowing fluid are:

1. The analysis is a basic approach to the problem proposed, an approach based on the actual physical situation. This is in contradistinction to the concept of the film heat transfer coefficient. This latter concept does provide rather easily attained, approximate answers to problems which cannot

wait for further advances in convective heat transfer analysis. However, the whole notion of the heat transfer coefficient is not an ideal means to a true understanding of the turbulent heat transport mechanism. For the film heat transfer coefficient is based on the fictitious model of a fluid with radially constant temperature and velocity, and of an abrupt temperature discontinuity at the fluid-solid boundary interface.

2. The differential equations, Eqs. 19 and 20, completely describe the coolant channel heat transfer system; at least they describe the system as well as the present level of turbulent heat transfer analysis allows. Moreover, means are presented for accounting for the peculiar geometry of the annulus.

3. The same differential equations, while embodying recent developments in the field, also serve as a framework for incorporating later advances in evaluating eddy conductivity. The original equations would be modified least if simple linear relationships were developed between eddy diffusivity for heat and eddy diffusivity for momentum, and between eddy conductivity in the radial direction and that in the axial direction.

4. The important role that eddy conductivity plays in the numerical calculations emphasizes the necessity for expanded laboratory investigation of this quantity. Ultimately sought are some generally applicable mathematical descriptions

of turbulent conductivity. Eddy conductivity in the radial direction has been the subject of a small amount of experimental work. As far as eddy conductivity in the axial direction is concerned, not even a qualitative discussion was found in the published literature.

5. The general development of the calculations casts serious doubt on the typical assumption of a negligible second derivative of temperature with respect to axial distance. In calculations for the specific case treated in Section V, this quantity (and its coefficient) affected axial temperature increments up to approximately eighteen percent.

VIII. RECOMMENDATIONS FOR FURTHER STUDY

The most important item of additional work has already been discussed in some detail. This is the matter of the programming effort to adapt the equations to a computer solution.

The bulk of this section will deal with improvements in the basic equations. These improvements will be directed principally toward a more realistic treatment of the fluid, that is, elimination of the constant properties assumption.

A refinement that requires no more analysis than what is presented in this paper but a great deal more in the way of calculation complexity is a direct sort of iteration. Solve the problem with fluid properties evaluated at the inlet temperature. As a second iteration, solve the functions P(r) and Q(r) (Eq. 27) with fluid properties evaluated at the temperature found at that particular x - r coordinate. This procedure will define a slightly different temperature distribution. This new distribution can then be the basis for a third iteration. The repetition can continue until the analyst is satisfied with the degree of convergence.

A more mathematically polished method of accounting for variable fluid properties would be to express this variability in the basic relationships, so that a first solution would fulfill the requirements of improved accuracy and avoid the clumsiness of the iterative method. The extreme complexity of the resultant equations cannot be discounted, but certain

tools are available to help in somewhat simplifying these equations. In this case, the derivatives in Eq. 12, the unsimplified heat balance, must be expanded in such a way that the variability of fluid properties with temperature is expressed. In such an equation many terms appear in the form $\partial f/\partial T$, where f is any one of the fluid properties. Some simplification is possible since terms of this type can be reasonably accurately replaced by a constant representing a straight line relationship with temperature. One serious restriction is that a given numerical value for this constant slope approximation is valid only for a specifically prescribed temperature range. For air this range should be less than two hundred Fahrenheit degrees. For plots to substantiate the assumption proposed, at least as far as air is concerned, see Humble et al. (11, p. 346). Pressurized water, and liquids in general, require a less broad range, certainly not more than one hundred degrees. For the variation of the properties of water, see the collection of plots in Eckert and Drake (8, pp. 262-265).

While pressures below the critical pressure have little influence over most of the fluid properties, a practicable method should be devised to account for pressure effects on density, particularly if the working fluid is a gas. Some further assistance in formulating a method dealing with a coolant of varying properties may be found in an investigation dealing solely with property changes in the radial direction

in a circular channel by Deissler and Eian (5).

A final correction could be made for compressibility effects. Some helpful ideas may be obtained from discussions by Durham (7) and by Deissler (4, pp. 25-26).

All these recommendations are in the direction of a more thorough mathematical analysis. Actually, the most noteworthy additional work would be done in the laboratory. The difficulties inherent in erecting a single annular channel, with attendant measuring and fluid transporting apparatus, with a varying heat load of accurately predictable variation are not to be gainsaid. However, such experimentation would not only test the present method and any eventual more refined analyses, but would supply data in an area long in need of additional reliable laboratory results.

IX. LITERATURE CITED

1. Barrow, H. Fluid flow and heat transfer in an annulus with heated core tube. Proc. Inst. of Mech. Engr. 169: 1113-1124. 1955.

2. Bird, R. B., Stewart, W. E., and Lightfoot, E. N. Transport phenomena. New York, N. Y., John Wiley and Sons, Inc. 1960.

3. Davis, E. S. Heat transfer and pressure drop in annuli. Amer. Soc. Mech. Engr. Trans. 65: 755-759. 1943.

4. Deissler, R. G. Analytical and experimental investigation of adiabatic turbulent flow in smooth tubes. U. S. National Advisory Committee for Aeronautics. Technical Note 2138. July, 1950.

5. _____ and Eian, C. S. Analytical and experimental investigation of fully developed turbulent flow of air in a smooth tube with heat transfer with variable fluid properties. U. S. National Advisory Committee for Aeronautics. Technical Note 2629. February, 1952.

6. _____ and Taylor, M. F. Analysis of fully developed turbulent heat transfer and flow in an annulus with various eccentricities. U. S. National Advisory Committee for Aeronautics. Technical Note 3451. May, 1955.

7. Durham, F. P. Pressure-temperature relation for constant-area compressible flow of a gas, considering heat transfer and friction with constant wall temperatures. U. S. Atomic Energy Commission Report LA-2129 [Los Alamos Scientific Laboratory, Los Alamos, N. M.] July, 1957.

8. Eckert, E. R. G. and Drake, R. M., Jr. Introduction to the transfer of heat and mass. 1st ed. New York, N. Y., McGraw-Hill Book Co., Inc. 1950.

9. Ferrari, C. Wall turbulence. U. S. National Aeronautics and Space Administration. Republication 2-8-59W. March, 1959.

10. Hall, W. B. Reactor heat transfer. Nuclear Engineering Monograph No. 3: 1-68. 1958.

11. Humble, L. V., Lowdermilk, W. H., and Desmon, L. G. Measurements of average heat-transfer and friction coefficients for subsonic flow of air in smooth tubes at high

surface and fluid temperatures. U. S. National Advisory Committee for Aeronautics. Report 1020. December, 1950.

12. von Kármán, T. Turbulence and skin friction. J. Aero. Sciences 1: 1-20. 1934.

13. Knudsen, J. G. and Katz, D. L. Fluid dynamics and heat transfer. New York, N. Y., McGraw-Hill Book Co., Inc. 1958.

14. Martinelli, R. C. Heat transfer to molten metals. Amer. Soc. Mech. Engr. Trans. 69: 947-959. 1947.

15. Mickley, H. S., Sherwood, T. K., and Reed, C. E. Applied mathematics in chemical engineering. 2nd ed. New York, N. Y., McGraw-Hill Book Co., Inc. 1957.

16. Monrad, C. C. and Pelton, J. F. Heat transfer by convection in annular spaces. Trans. Amer. Inst. Chem. Engr. 38: 593-608. 1942.

17. Reichardt, H. Principles of turbulent heat transfer. U. S. National Advisory Committee for Aeronautics. Technical Memorandum 1408. September, 1957.

18. Rothfus, R. R., Monrad, C. C., and Senecal, V. E. Velocity distribution and fluid friction in smooth concentric annuli. Ind. and Engr. Chem. 42: 2511-2520. 1950.

19. _____, _____, Sikchi, K. G., and Heideger, W. J. Isothermal skin friction in flow through annular sections. Ind. and Engr. Chem. 47: 913-918. 1955.

20. Schlichting, H. Boundary layer theory. 4th ed. New York, N. Y., McGraw-Hill Book Co., Inc. 1960.

21. Tribus, M., Noyes, R. N., and Norris, R. H. Temperature distribution for turbulent flow through annuli with any chosen axial variation of heat flux over each of the two walls. U. S. Atomic Energy Commission Report AECU-3938 [General Electric General Engineering Laboratory, Schenectady, N. Y.] November, 1955.

X. ACKNOWLEDGEMENT

The author is indebted to his major professor, Dr. Donald F. Young. Dr. Young's professional competence proved a reliable source of guidance and good judgment. Furthermore, his intellectual curiosity was a constant stimulus through the course of this investigation.

The author also expresses his thanks to his wife, Judith, for her assistance, for her helpful criticisms, and for her patience during this effort.